Hall Sensor Array based Magnetic Field Measurement System

Submitted in partial fulfillment of the requirements

of the degree of

Bachelor of Engineering

in

Electronics and Telecommunication Engineering

by

Name	Roll No.
Ms. Annabelle Dani	**301406**
Ms. Monika Budania	**301411**
Ms. Sanika Itagi	**301422**
Mr. Lawansh Singh	**301458**

Supervisors:

External Guide: Dr. B. Satyanarayana
Internal Guide: Mrs. Amruta Pabarekar

Department of Electronics and Telecommunication Engineering

Fr. Conceicao Rodrigues Institute of Technology, Vashi

UNIVERSITY OF MUMBAI

2017-18

टाटा मूलभूत अनुसंधान संस्थान
TATA INSTITUTE OF FUNDAMENTAL RESEARCH
होमी भाभा रोड, कोलाबा, मुंबई – ४०० ००५.
Homi Bhabha Road, Colaba, Mumbai - 400 005.
परमाणु ऊर्जा विभाग की स्वायत्त संस्था
भारत सरकार एवं समविश्वविद्यालय
An Autonomonus Institution of the Department of Atomic Energy
Government of India and Deemed University

दूरभाष / Telephone : +91 22 2278 2000
फैक्स / Fax : +91 22 2280 4610 / 11

वेबसाईट / Website : www.tifr.res.in

Project Report Approval

To,
Dr. Milind Shah,
Head of EXTC Department,
Fr.C.R.I.T, Vashi.

This is to certify that Annabelle Dani (301406), Monika Budania (301411), Sanika Itagi (301422) and Lawansh Singh (301458) from EXTC Department have successfully completed their B.E Project titled Hall Sensor Array based Magnetic Field Measurement System in TIFR under the Guidance of Dr. B. Satyanarayana in academic year 2017-2018.

Dr. B. Satyanarayana

Project Report Approval for B.E

This project report **Hall Sensor Array based Magnetic Field Measurement System** by **Annabelle Dani (301406), Monika Budania (301411), Sanika Itagi (301422)** and **Lawansh Singh (301458)** is approved for the degree of **Bachelor of Engineering** in **Electronics and Telecommunication** of **University of Mumbai**.

Examiners:

1. _____

2._____

Supervisors:

1._____

2._____

Date:

Place:

Declaration

We declare that this written submission represents our ideas in our own words and where others' ideas or words have been included, we have adequately cited and referenced the original sources. We also declare that we have adhered to all principles of academic honesty and integrity and have not misrepresented or fabricated or falsified any idea/data/fact/source in our submission. We understand that any violation of the above will be cause for disciplinary action by the Institute and can also evoke penal action from the sources which have thus not been properly cited or from whom proper permission has not been taken when needed.

(Annabelle Dani 301406)

(Monika Budania 301411)

(Sanika Itagi 301422)

(Lawansh Singh 301458)

Date:

Place:

Annabelle Dani, Monika Budania, Sanika Itagi, Lawansh Singh, External Guide: B. Satyanarayana., Internal Guide: Mrs. Amruta Pabarekar, Title: ―Hall Sensor Array based Magnetic Field Measurement System, B.E. Semester VIII, Final Year Project Report, Department of Electronics & Telecommunication Engineering, Fr.C.R.IT, Vashi, April 2018.

Abstract

Measurement of magnetic fields is one of the important requirements in many research and development applications. Hall Sensors which function on the principle of Hall Effect, are used to measure these parameters. This project aims to propose a Hall sensor array based magnetic field measurement system.16 hall sensors are mounted on a thin mount equidistant to each other at a gap of 60 mm and their sensing element being parallel to the mount. While on the front-end, the sensor signals are multiplexed and amplified, they are digitized and processed by a microcontroller on the back-end. A suitable graphical user interface is also developed to customize and control the system as well to output and archive the data suitably. This magnetic field measurement system is for a specific application i.e. INO project, but due to its low cost and modularity, it can be extended to the civilian applications where these sensors can be used in research institutions and industries.

Contents

List of Figures

List of Tables

List of Abbreviations

Abbreviation	Term
INO	Indian Neutrino Observatory
ICAL	Iron Calorimeter
RPC	Resistive Plate Chambers
SQUID	Super Conducting Quantum Interference Device
LabVIEW	Laboratory Virtual Instrument Engineering Workbench
FPGA	Field Programmable Gate Arrays
DSP	Digital Signal Processor
IDE	Integrated Design Environment
EAGLE	Easily Applicable Graphical Layout Editor
ECR	Electron cyclotron resonance
VISA	Virtual Instrument Software Architecture

Chapter 1

INTRODUCTION

Magnetic field vector is a force generated by moving electric charges currents and calculated using Ampere's Law or Biot-Savart Law. When describing it inside magnetized materials which themselves contribute to internal magnetic fields, this field is denoted by either magnetic flux density, B (Tesla) or magnetic field strength, H (amperes per meter). Magnetic field is one of the two components of the Electromagnetic force, which is one of the most pervasive fundamental forces of nature. Magnetic fields are most commonly applied in working of modern technologies and designing instruments. Motors and generators, electromotive instruments and mass transport systems, navigation devices and material handling equipment's are some of the examples. While in everyday life, magnetic fields created by permanent magnets are most often encountered, magnets of different kinds - electromagnetic, superconducting etc., are being extensively used in experimental nuclear and high energy physics and material sciences. Very large and powerful magnets are used to build particle accelerators and detectors typically to accelerate or bend the charged particle beams and measure the energy of the particles. Magnetic forces give information about the charge carriers in a material through the Hall Effect. And on the other hand, Hall Effect is often exploited to precisely measure and monitor magnetic field strengths of all the magnetic systems mentioned above, which is an important requirement of such systems. The idea is to build a prototype of

magnetic field measurement system which would be useful on a small scale at INO project for studying neutrinos and in laboratories to study magnetic fields.

1.1 Problem Overview

The India-based Neutrino Observatory (INO) is a multi-institutional national project aimed at building a world-class underground laboratory at the Bodi West Hills near Madurai in Tamil Nadu. The collaboration is deeply engaged in design and construction of a mega science experiment called Iron Calorimeter (ICAL) for studying many key open questions involving the elusive particles, neutrinos. The magnetized ICAL will consist of more than 50000 tons of iron plates arranged in stacks with gaps in between where around 28,800 Resistive Plate Chambers (RPCs) would be inserted as active detectors. A total of about 3.6 million ultra-high-speed detector signals need to be instrumented in this detector [1].

One of the most important capabilities of the ICAL detector is to distinguish between positively and negatively charged particles produced by the neutrinos within the ICAL detector as well as measure their energies. In fact, ICAL will be world's largest electromagnet, which is built using the iron plates and copper coils. About 1.5 Tesla magnetic field which will be produced within the ICAL will bend the particles of opposite polarities in different directions, hence identifying their charge. Also, by measuring the radius of curvature of these bent tracks; one can estimate the momentum or energy of the particles. Therefore, there's a need for precise simulation of the field within the volume of the detector as well as its measurement.

It is proposed by the INO collaboration that a prototype ICAL detector of 4m x 4m x 11 layers and weighing about 85 tons be built in IICHEP laboratory in Madurai to facilitate initial experiments related to magnet construction and other concerned issues. A picture of this magnet under construction is shown in the below Figure. Construction scheme of the magnet along with iron plates and copper coils is clearly seen in the picture.

Fig.1.1 Magnet of the prototype ICAL detector under installation and commissioning in Madurai.

Simulated magnetic flux in a layer of the prototype detector using the configuration shown in Fig 1.1 is given in Fig 1.2. The design criteria is that we achieve more than 1 Tesla field in as large a volume (about 90%) as possible using minimum current in the Copper coils.

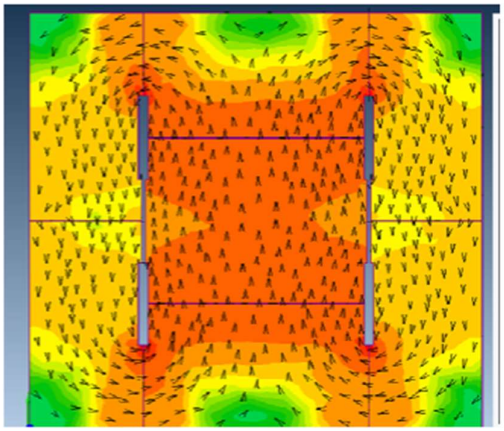

Fig.1.2 Simulated magnetic flux lines in an iron layer of prototype detector.

It was strongly desired by the Collaboration that a reliable and versatile measurement system may be developed for insitu monitoring the magnetic field in the prototype detector of the ICAL.Also if this system is found to be useful then multiple units of the designed board may be created and used in ICAL.

1.2 Research Objective

The objective of this research work is:

i. To make a prototype of the magnetic field measurement system which would be a part of the study for the India based Neutrino Observatory (INO) project.
ii. To build a magnetic field measurement system with the help of arrays (numbers:16) of hall sensors on a thin PCB strip.
iii. To read and store all the data signals and analyze the same for calibration of the system.

1.3 Report Outline

Chapter 2 provides literature survey of fundamental particles like neutrinos and phenomenon such as Hall Effect.

Chapter 3 discusses the proposed system and overall flow of the project and its implementation.

Chapter 4 gives the details of the results obtained while testing the system components and explains the designing and implementation of the work achieved till date.

Chapter 5 summarizes and concludes the results obtained until date in all the segments and also describes the future work.

Appendix I comprises all the course outcomes that are relevant to the project and hence the program outcomes we have achieved while doing the project.

Appendix II comprises the datasheets of the integrated circuits used in this project.

Chapter 2

LITERATURE SURVEY

The literature survey consists of initial study topics which are given below:

2.1 Neutrinos

Neutrinos are subatomic particles produced by the decay of radioactive elements and are elementary particles that lack an electric charge [2]. They are denoted by the Greek letter ν. The neutrino is so named because it is electrically neutral and because its rest mass is so small that it was originally thought to be zero. The weak force has a very short range, gravity is extremely weak on the subatomic scale, and neutrinos do not participate in the strong interaction. Thus, neutrinos typically pass through normal matter unimpeded and undetected [3].

Neutrinos are tiny elementary particles like the electron but not part of the atom. Neutrinos are abundantly found in nature. The Sun, the stars and the atmosphere produce millions of neutrinos every second. Most of these neutrinos pass through our body and we do not realize it. They can even pass through the earth and come out on the other side. The reason they can do this is because they interact very less and studying these particles in the laboratory is extremely difficult.

Many properties and characteristics of neutrinos are not known to humanity. Thus, research on these particles will yield extremely useful information. These particles can make a lot of phenomena clear to us from everything like the birth of the universe to the nuclear reactions that power our cities and therefore they are an important area of scientific studies [3].

2.2 The Hall Effect

The Hall Effect is the production of a voltage difference (Hall voltage, V_H) across an electrical conductor, transverse to an electric current in the conductor and to an applied magnetic field perpendicular to the current. It was discovered by Edwin Hall in 1879 [4].

The Hall Effect is due to the nature of the current in a conductor. Current consists of the movement of many small charge carriers, typically electrons, holes, ions or all three. When a magnetic field is present, these charges experience a force, called the Lorentz force. The Lorentz force is the combination of electric and magnetic force on a point charge due to electromagnetic fields. A particle of charge *q* moving with velocity v in the presence of an electric field E and a magnetic field B experiences a force F [5].

F = qE + qv x B _____ (I) [5]

When a magnetic field is absent, the charges flow in an approximately straight, line of sight paths between collisions with impurities, phonons, etc.

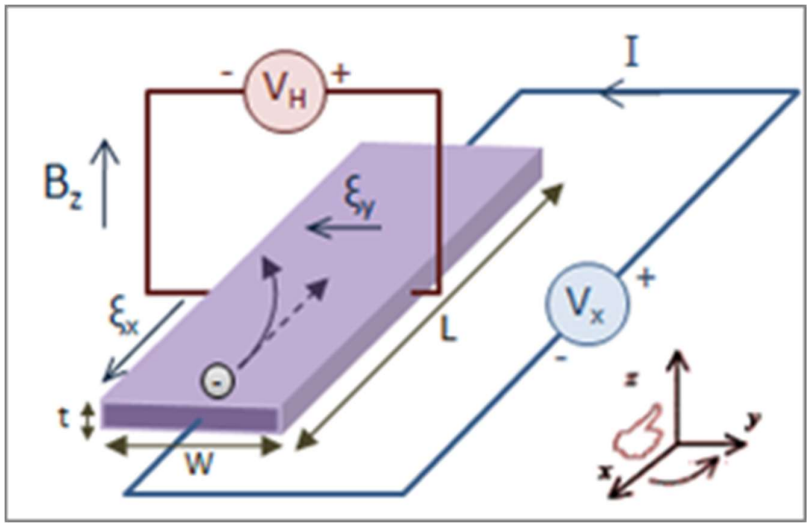

Fig.2.1 Sketch of Hall Generator [4]

When a magnetic field with a perpendicular component is applied, their paths between collisions are curved, (following the solid, curved arrow) thus moving charges accumulate on one face of the material (left side). This leaves equal and opposite charges exposed on the other face (right side), where there is a scarcity of mobile charges. This creates an electric field ξ_y in the direction of the assigned V_H. V_H is negative for some semi-conductors where "holes" appear

to flow. In steady state, ξ_y will be strong enough to exactly cancel out the magnetic force, thus the electrons follow the straight arrow (dotted line). The result of leaving equal and opposite charges on both faces of the material is an asymmetric distribution of charge density across the Hall element, arising from a force that is perpendicular to both the 'line of sight' path and the applied magnetic field. The separation of charge establishes an electric field that opposes the migration of -further charge, so a steady electric potential is established for as long as the charge is flowing.

In the steady state, F=0. Also, E is assigned in the y-direction. So, from equation (I).we get,

$$\mathbf{0 = E_y - v_x B_z}$$

$$\mathbf{E_y = v_x B_z \_\_\_\_\_ (II)} \text{ [5]}$$

In wires, electrons flow instead of holes, so $\mathbf{v_x \Rightarrow - v_x}$ and $\mathbf{q \Rightarrow - q}$.

Also, $\mathbf{E_y = -V_H / \omega}$. So in equation (II),

$$\mathbf{V_H = v_x B_z \omega}$$

Solving for ω we get Hall voltage as,

$$\mathbf{V_H = I_x B_z / (nte)}$$

Where, $\mathbf{I_x}$ = current in the negative direction of the electron current

n = charge carrier density

t = height of the material

-e = charge of each electron

The Hall coefficient, $\mathbf{R_H}$, is defined as the ratio of the induced electric field to the product of the current density and the applied magnetic field and is given by[5],

$$\mathbf{R_H = E_y / j_x B_z}$$

Where, j = current density of the carrier electrons

In SI units,

$$\mathbf{R_H = E_y / j_x B = V_H t / I B = -1 / ne \_\_\_\_\_ (III)} \text{ [5]}$$

The units of R_H are usually expressed as m^3/C, or Ω·cm/G, or other variants. As a result, the Hall effect is very useful as a means to measure either the carrier density or the magnetic field [4].

2.3 Hall Effect Sensors

Magnetic sensors are used for converting magnetic field into electrical signals [6]. These sensors have wide range of applications such as detection, discrimination and localization of ferromagnetic and conducting objects, navigation, position tracking and antitheft systems. Possible magnetic field measurement methods found in the literature are induction based (flux meter and flux gate), Hall Effect based, magneto resistance based, magnetic resonance based and super conducting quantum interference device (SQUID) based. But methods like SQUID come under low field sensors which can sense very low values of magnetic fields, i.e., under 1μGauss. Hall sensors have very wide range, good accuracy and a very wide bandwidth, so they were chosen as the primary sensors for magnetic field measurement system for the ICAL prototype detector.

Most commonly used magnetic sensors are MEMS-type, which are bigger in size. In this project, size of the probe is of major concern, where the thickness of the mount including the sensor should fit into a slot of less than 3mm. Therefore, a Hall sensor is chosen. A hall sensor is a type of magnetic sensor whose output is a function of magnetic field density. It is based on the principle of Hall Effect, discovered in 1879 by Edwin Hall. The Hall Effect is favored in materials with high electron mobility and low conductivity [7].

2.3.1 Working Principle

When a beam of charged particles passes through a magnetic field, forces act on the particles and the beam is deflected from a straight path. The flow of electrons through a conductor is known as a beam of charged carriers. When a conductor is placed in a magnetic field perpendicular to the direction of the electrons, they will be deflected from a straight path. As a consequence, one plane of the conductor will become negatively charged and the opposite side will become positively charged. The voltage between these planes is called the Hall voltage [7].

When the force on the charged particles from the electric field balances the force produced by magnetic field, the separation of them will stop. If the current is not changing, then the Hall voltage is a measure of the magnetic flux density. Basically, there are two kinds of Hall Effect sensors. One is linear which means the output of voltage linearly depends on magnetic flux

density; the other is called threshold which means there will be a sharp decrease of output voltage at each magnetic flux density.

From equation (III) we have,

$$V_H = R_H \left(\frac{I}{t} \times B\right) \quad [7]$$

Where, V_H is the Hall Voltage in volts

R_H is the Hall Effect co-efficient

I is the current flow through the sensor in amps

t is the thickness of the sensor in mm

B is the Magnetic Flux density in Tesla

There are two types of Hall Effect sensors, one providing analog output and the other digital output. The analog sensor is composed of a voltage regulator, a Hall Element and an amplifier. We can see that the output of the sensor is analog and proportional to the Hall Element output or the magnetic field strength. These types of sensors are suitable and used for measuring proximity because of their continuous linear output [8]. Linear or analogue sensors give a continuous output voltage that increases with a strong magnetic field and decreases with a weak magnetic field.

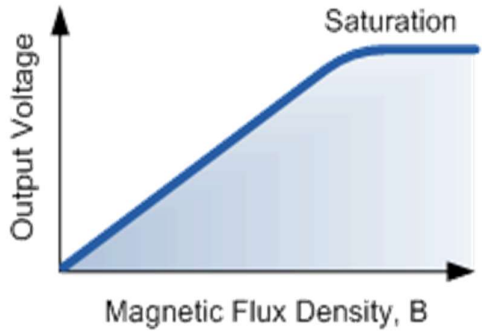

Fig.2.2 Analog output of Hall Effect sensor [1]

The above figure shows that in linear output Hall Effect sensors, as the strength of the magnetic field increases the output signal from the amplifier will also increase until it begins to saturate by the limits imposed on it by the power supply. Any additional increase in the magnetic field will have no effect on the output but drive it more into saturation [8].

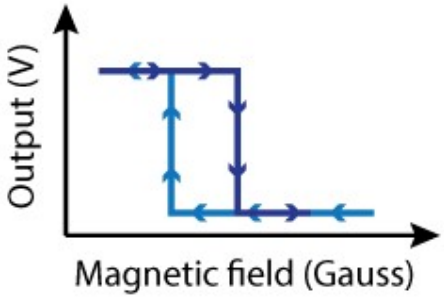

Fig.2.3 Digital output of Hall Effect sensor [8]

On the other hand, the digital output sensors provide just two output states, either "ON" or "OFF". These types of sensors have an additional element that is the Schmitt Trigger which provides hysteresis or two different thresholds levels so the output is either high or low.

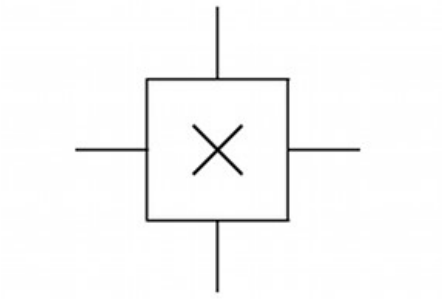

Fig.2.4 Circuit symbol of Hall sensor [8]

2.3.2 Applications

Some applications of the Hall sensor are:

1. Position sensing: Sensing the presence of magnetic objects (connected with the position sensing) is the most common industrial application of Hall Effect sensors, especially those operating in the switch mode (on/off mode). The Hall Effect sensors are also used in the brushless DC motor to sense the position of the rotor and to switch the transistors in the right sequence.

2. Smartphones use hall sensors to determine if the flip cover accessory is closed.

3. Direct current (DC) transformers: Hall Effect sensors may be utilized for contactless measurements of DC current in current transformers. In such a case the Hall Effect sensor is mounted in the gap in magnetic core around the current conductor. As a

result, the DC magnetic flux can be measured, and the DC current in the conductor can be calculated.

4. Automotive fuel level indicator: The Hall sensor is used in some automotive fuel level indicators. The main principle of operation of such indicator is position sensing of a floating element. This can either be done by using a vertical float magnet or a rotating lever sensor.
    - In a vertical float system, a permanent magnet is mounted on the surface of a floating object. The current carrying conductor is fixed on the top of the tank lining up with the magnet. When the level of fuel rises, an increasing magnetic field is applied on the current resulting in higher Hall voltage. As the fuel level decreases, the Hall voltage will also decrease. The fuel level is indicated and displayed by proper signal condition of Hall voltage [9].

2.3.3 Specifications of Hall Probe

Table 2.1 lists specifications of the measurement system.

Table.2.1 Hall sensor specifications [10]

Parameter	Value
Basic Sensor Material	Mono-crystal GaAs
Type of Probe	For transverse field measurement
Measurement Range	Upto 30 KGauss
Accuracy	0.2% of full scale
Non Linearity	<1%
Maximum Input current/voltage	30 mA/10 V
Max input power	150 mW
Operating Temp. Range	40-150 °C
Hall output voltage at B=100mT, I=8 mA, V=6V	110-150 mV
Offset Voltage	±11 mV
Input Resistance	650-800 Ω
Output Resistance	650-800 Ω
Temperature Coefficient of Hall output voltage	0.06%/°C
Temperature Coefficient of Hall output resistance	0.3%/°C

2.4 Softwares

An introduction to the software's that are used for implementation of the proposed system has been discussed below

2.4.1 Proteus Design Suite

Proteus Design Suite is a proprietary software tool suite used primarily for .It is a simulation and design software tool developed by Lab center Electronics for Electrical and Electronic circuit design. The software is used mainly by electronic design engineers and electronic technicians to create electronic schematics and electronic prints for manufacturing printed circuit boards (PCBs). Proteus combines ease of use with powerful features to help design, test and layout PCBs. It is one of the most complete electronic tool packs on the market as it allows us to create PCBs from our PCs. It has nearly 800 microcontroller variants ready for simulation straight from the schematic and is one of the most intuitive professional PCB layout packages on the market. It also integrates tools with which we can design and simulate within the Arduino environment. This is extremely useful as the Arduino Board is one of the most popular boards at present [11].

2.4.2 EAGLE

EAGLE is a scriptable electronic design automation application with schematic capture, printed circuit board layout, auto-router and computer-aided manufacturing features. EAGLE stands for Easily Applicable Graphical Layout Editor and is developed by Cad Soft Computer GmbH. Cad soft Computer GmbH was acquired by Autodesk Inc. in 2016 [12].

The commercial licenses range from one schematic sheet, two signal layers, and a 100x80mm routing area to the Ultimate license with 16 signals and a four meter square routing area. For non-commercial licenses, the free educational edition features 99 schematic sheets, six signal layers, and a 160x100mm routing area [12].

Features of EAGLE [12]:

- The PCB layout editor allows back annotation to the schematic and auto-routing to automatically connect traces based on the connections defined in the schematic
- EAGLE saves Gerber and PostScript layout files and Excel on and Side & Meyer drill files. These standard files are accepted by many PCB fabrication companies
- Available for Windows, Mac and Linux.

- EAGLE contains a schematic editor, for designing circuit diagrams. Parts can be placed on many sheets and connected together through ports.

2.4.3 OrCAD

OrCAD is a proprietary software tool suite used primarily for electronic design automation (EDA). The software is used mainly by electronic design engineers and electronic technicians to create electronic schematics and electronic prints for manufacturing printed circuit boards. The name OrCAD is a portmanteau, reflecting the company and its software's origins: Oregon + CAD. OrCAD is a suite of products for EDA, and includes a schematic editor (Capture), a circuit simulator (PSpice) and a PCB designer [13]. OrCAD PCB Designer is a printed circuit board designer application, and part of the OrCAD circuit design suite Designer includes various automation features for PCB design, board-level analysis and design rule checks (DRC). The PCB design may be accomplished by manually tracing PCB tracks or using the Auto-Router provided. Such designs may include curved PCB tracks, geometric shapes, and ground planes.

PCB Designer integrates with OrCAD Capture, using the component information system (CIS) to store information about a certain circuit symbol and its matching PCB footprint

2.4.4 LabVIEW

LabVIEW, short for Laboratory Virtual Instrument Engineering Workbench, is a programming environment in which you create programs using a graphical notation (connecting functional nodes via wires through which data flows); in this regard, it differs from traditional programming languages like C, C++, or Java, in which you program with text. However, LabVIEW is much more than a programming language. It is an interactive program development and execution system designed for people, like scientists and engineers, who need to program as part of their jobs. The LabVIEW development environment works on computers running Windows, Mac OS X, or Linux. LabVIEW can create programs that run on those platforms, as well as Microsoft Pocket PC, Microsoft Windows CE, Palm OS, and a variety of embedded platforms, including Field Programmable Gate Arrays (FPGAs), Digital Signal Processors (DSPs), and microprocessors [14].

As a step toward industry-wide software compatibility, NI developed one specification for I/O software—the Virtual Instrument System Architecture, or VISA. The VISA specification defines a next-generation I/O software standard for GPIB, Serial, and other interfaces. VISA unifies the industry to make software interoperable, reusable, and able to stand the test of time. The VISA package enables the different microcontrollers to communicate with the system serially over COM ports or RS-232 communication interfaces.

2.4.5 Arduino IDE

The open-source Arduino Integrated Development Environment (IDE) makes it easy to write code and upload it to the board [15]. It runs on Windows, Mac OS X, and Linux. The environment is a cross-platform application written in Java and based on Processing and other open source software. This software can be used with any Arduino board. It is designed to introduce programming to artists and other newcomers unfamiliar with software development. It includes a code editor with features such as syntax highlighting, brace matching, and automatic indentation, and is also capable of compiling and uploading programs to the board with a single click. A program or code written for Arduino is called a “sketch". Arduino programs are written in C or C++. The Arduino IDE comes with a software library called "Wiring" from the original Wiring project, which makes many common input/output operations much easier. The Arduino IDE uses the GNU tool chain and AVR Lib to compile programs. As the Arduino platform uses Atmel microcontrollers, Atmel's development environment, AVR Studio or the newer Atmel Studio, may also be used to develop software for the Arduino. Arduino also simplifies the process of working with microcontrollers, but it offers some advantage for teachers, students, and interested amateurs over other systems:

- Inexpensive - Arduino boards are relatively inexpensive compared to other microcontroller platforms.
- Cross-platform - The Arduino software runs on Windows, Macintosh OSX, and Linux operating systems. Most microcontroller systems are limited to Windows.
- Simple, clear programming environment - The Arduino programming environment is easy-to-use for beginners, yet flexible enough for advanced users to take advantage of as well. For teachers, it's conveniently based on the Processing programming environment, so students learning to program in that environment will be familiar with the look and feel of Arduino.

- Open source and extensible software- The Arduino software is published as open source tools, available for extension by experienced programmers.

2.4 System components

2.4.1 IC MC14067BCP

The MC14067 multiplexer/demultiplexer is a digitally controlled analog switch featuring low ON resistance and very low leakage current. This device can be used in either digital or analog applications. The MC14067 is a 16−channel multiplexer/demultiplexer with an inhibit and four binary control inputs A, B, C, and D. These control inputs select 1−of−16 channels by turning ON the appropriate analog switch [16].

Features

- Low OFF Leakage Current
- Matched Channel Resistance
- Low Quiescent Power Consumption
- Low Crosstalk Between Channels
- Wide Operating Voltage Range: 3 to 18 V
- Low Noise

Table.2.2. Truth Table of MC14067BCP [16]

Control Inputs					Selected Channel
A	B	C	D	Inh	
X	X	X	X	1	None
0	0	0	0	0	X0
1	0	0	0	0	X1
0	1	0	0	0	X2
1	1	0	0	0	X3
0	0	1	0	0	X4
1	0	1	0	0	X5
0	1	1	0	0	X6
1	1	1	0	0	X7
0	0	0	1	0	X8
1	0	0	1	0	X9
0	1	0	1	0	X10
1	1	0	1	0	X11
0	0	1	1	0	X12
1	0	1	1	0	X13
0	1	1	1	0	X14
1	1	1	1	0	X15

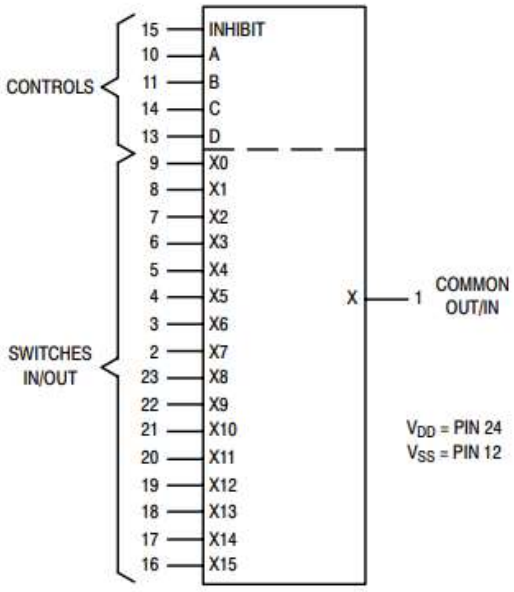

Fig.2.5.MC14067BCP Pin configuration [16]

2.4.2 IC LM747N

The LM747 is a general purpose dual operational amplifier. The two amplifiers share a common bias network and power supply leads. Otherwise, their operation is completely independent. Additional features of the LM747 are: no latch-up when input common mode range is exceeded, freedom from oscillations, and package flexibility [17].

Features

- No frequency compensation required
- Short-circuit protection
- Wide common-mode and differential voltage ranges
- Low power consumption

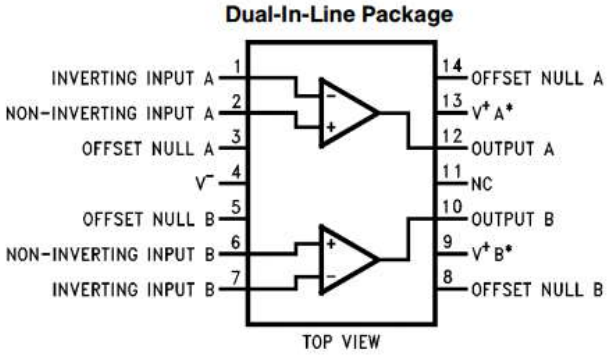

Fig.2.6 LM747 Pin configuration [17]

2.5.3. Arduino UNO

Arduino Uno is a microcontroller board based on the ATmega328P. It has 14 digital input/output pins (of which 6 can be used as PWM outputs), 6 analogue inputs, 16MHz quartz crystal, a USB connection, a power jack, an ICSP header and a reset button. It contains everything needed to support the microcontroller; simply connect it to a computer with a USB cable or power it with a AC to DC adapter or battery to get started [18].

Table2.3. Technical specifications of Arduino Uno Board [18]

Micro-controller	ATmega328P
Operating voltage	5V
Input voltage (recommended)	7-12 V
Input voltage (limit)	6-20 V
Digital i/o pins	14 (of which 6 provide PWM output)
PWM digital I/O pins	6
Analog input pins	6
DC current per I/O pin	20 mA
DC current per 3.3 V pin	50 mA
Flash memory	32 KB
SRAM	2 KB
EEPROM	1 KB
Clock Speed	16 MHz
LED built in	13

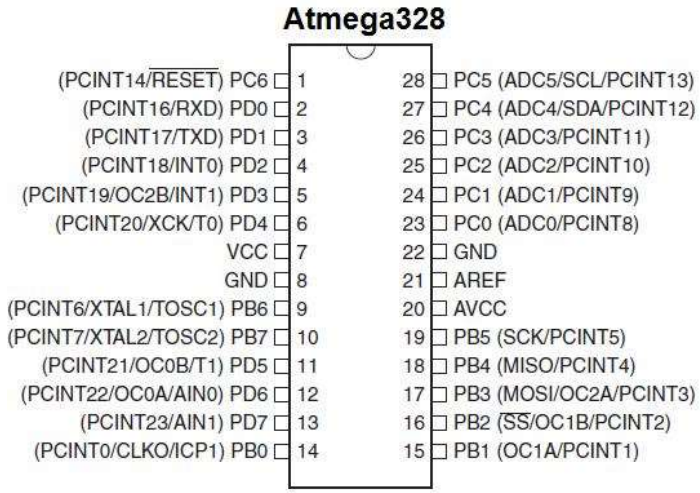

Fig.2.7 Atmega328 Pin configuration [19]

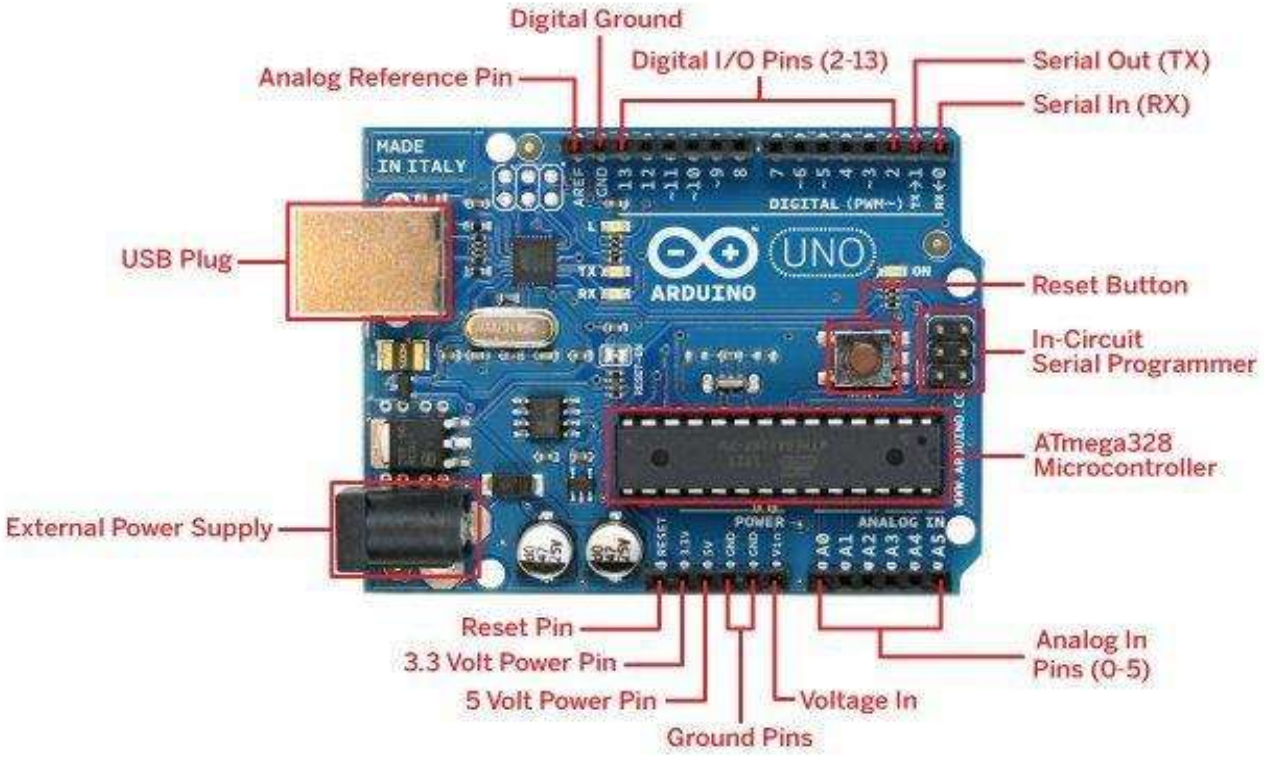

Fig.2.8 Arduino Uno Board

2.5.4 ECR ION SOURCE

The testing part of the system was done with the help of ECR ion source machine in TIFR. The Electron cyclotron resonance (ECR) ion source at TIFR consists of a Cu plasma chamber. It is a permanent magnet (SmCo Permanent) ECR ion source with dipolar axial and closed structure hexapolar radial magnetic fields. Field maxima at the ends are 0.8 and 1.1 T. The magnetic field has a minimum at the center of the plasma chamber; therefore, it is known as the min-B configuration. The MW frequency is 14.5 GHz with 500 W maximum output. At this frequency, the resonance magnetic field turns out to be 0.51 tesla. A plasma chamber contains an insulated metal rod (called the bias rod). The maximum extraction voltage is 30 kV. Gases are introduced in the plasma chamber by two electrically controlled gas inlet valves. Extracted ions are focused by an electrostatic Einzel lens. A 90◦ bending dipole magnet (0.3 tesla) analyzes the charge state of ions. ECR ion sources produce high dosage of x-ray radiation and hence, to avoid radiation exposure, the high-voltage (HV) deck has been covered with aluminum-covered lead shields.

A LabVIEW-based command and control system developed. Field-point modules along with the controller are mounted on the high voltage deck. The dipole magnet, extraction voltage, Einzel lens, bias rod and gas flow controller channels are controlled through the NI FP AO-200 analogue output module channels. The magnet current, extraction and Einzel lens voltages, Faraday cup current, ECR body temperature and micro-wave tuner position were monitored with the FP AI-110 analogue input module channels. All the field-point modules are cascaded to the FP-2000 real-time controller and connected to the wireless access point kept on the high voltage deck. The PC is also connected through the wireless router. All the control and monitoring parameters of the source are transmitted and received through this wireless mode [20].

Fig.2.9 ECR Ion source Machine [20]

2.5.5 CYSJ106C

CYSJ106C series Hall-effect element is a ion-implanted magnetic field sensor made of monocrystalline gallium arsenide (GaAs) semiconductor material group III-V using ion implanted technology. It can convert a magnetic flux density signal linearly into voltage output [21].

FEATURES

- High Linearity
- Superior Temperature Stability
- Miniature Package

- Wide measuring range 0-3T

TYPICAL APPLICATION

- Magnetic Field Measurement
- DC Brushless Motor
- Current Sensor
- Non-contact Switch
- Position Control

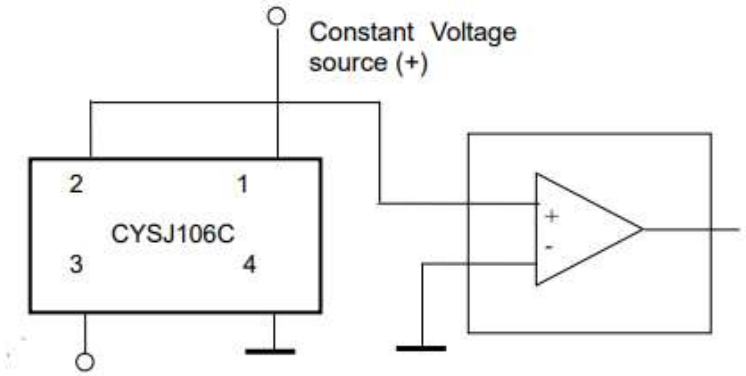

Fig.2.10 Pin Configuration of CYSJ106C [21]

Pin 1: positive input voltage V+.

Pin 3: negative input voltage V-

Pin 2: OUTPUT

Pin 4: GND

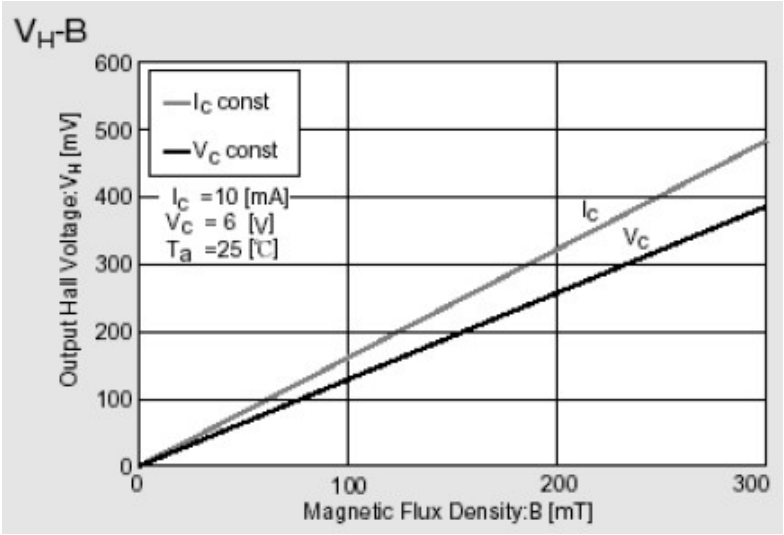

Fig.2.11 Output Characteristics of Hall Sensor [21]

The figure 2.11 shows the variation of hall voltage with increasing magnetic field. This can also be referred to calibrate the final probe. The slope of this curve is about 7.5 G/mV, which needs to match with the slope that will be obtained in calibration results. The corresponding test conditions have been provided. This graph is referred from CYSJ106C datasheet which is attached in annexure 1.

Chapter 3

SYSTEM DESCRIPTION AND IMPLEMENTATION

This chapter deals with the hardware implementation of Hall Sensor based Magnetic Measurement System. The measurement system essentially comprises of three major subsystems, namely the signal acquisition, analog and digital signal processing and front end data and user interface. The signal acquisition subsystem senses the magnetic field at multiple points in and converts it into corresponding analog voltages. This is essentially achieved by the network of a 16 Hall sensors, which in turn are fed to the subsequent analog and digital signal processing subsystems. The signals from the 16 Hall sensors are multiplexed and sent to the analog to digital converter (ADC) of a microcontroller for digitization, after amplification by an operational amplifier. Overall control, readout and communication with the front end user interface are achieved a commercial microcontroller board. The front-end GUI refreshes the display screen with the acquired data after a fixed time. The multiplexing avoids need for one ADC channel of the microcontroller per sensor, instead only one ADC channel is sufficient for all the 16 sensors.

3.1 System Description

The system consists mainly of an array of 16 Hall sensors placed 60mm from each other, connected together by a single wire for each of the +V, -V and GND terminals. The outputs of

the Hall sensors have separate wires and are connected independent of each other. Thus, there are 16 wires for each of the 16 Hall sensor outputs and 3 wires for the power supply connections of the array, i.e., a total of 19 wires that are connected to the PCB which holds the amplifier and buffer stage of the system. The PCB output, which is the 16:1 multiplexed output of all the Hall sensors is then passed into the Arduino Uno board. The Arduino board is interfaced with LabVIEW and the front panel is shown on this software with all resulting values.

3.2 System Implementation

The first step in the implementation of the system was to understand what exactly was required of the system and what parameters were to be considered in its design. As mentioned before, the array consists of 16 Hall sensors and the system is to be designed to fit in between consecutive iron plates. The array is planned to be inserted or mounted in the gaps of size 1000mm x 56mm x 3mm available in the structure.

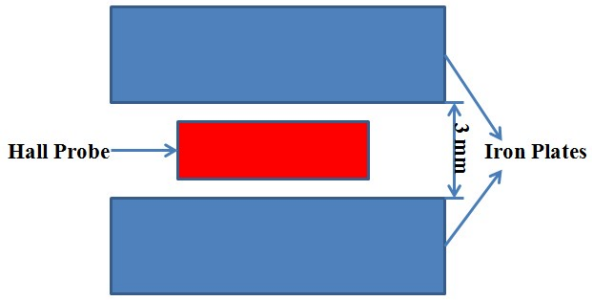

Fig.3.1 Schematic of sensor position and placement in the detector.

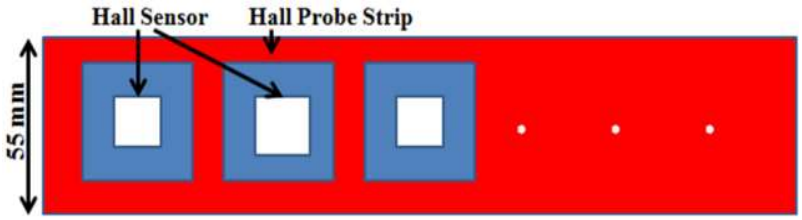

Fig.3.2 Schematic of Hall probe array

Hence, it was important to identify those components that were best suited to the requirements specified and that were of the appropriate size required in this system. The specifications are mentioned in Table 2.1. Accordingly, Hall sensor data sheets were studied and the two ICs closest to the given specifications were shortlisted. The two shortlisted Hall sensors were

CYSJ106C and CYSJ166A, both of which are of thickness 0.6mm which meets the basic requirement of fitting into the 3mm gap between the iron plates. The specifications of both these sensors are shown below.

Table.3.1. CYSJ106C & CYSY166A sensor specifications

Sr. No.	Parameters	CYSJ106C	CYSJ166C
1.	Basic Sensor Material	Mono-crystal GaAs	Mono-crystal GaAs
2.	Type of probe	For transverse field measurement	For transverse field measurement
3.	Measurement Range	Up to 30kGauss (3T)	Up to 30kGauss (3T)
4.	Maximum input current/voltage	13mA/10V	12V
5.	Maximum input power	150mW	150mW
6.	Operating temperature range	-40 to 125°C	-40 to 125°C
7.	Hall output voltage at B=100mT, I=8mA, V=6V	110-150mV	156-204mV
8.	Offset voltage	±11mV	±8mV
9.	Input resistance	650-800Ω	1000-1500Ω
10.	Output resistance	650-800Ω	1800-3000Ω
11.	Temperature co-efficient of Hall output voltage	-0.06% / °C	-0.06% / °C
12.	Temperature co-efficient of input output resistance	0.3% / °C	0.3% / °C

3.3 Hardware implementation

The next part of the implementation was to design the amplifier and buffer stage circuit. Three possible designs were considered and the selected design was modified as per the decided components. The three circuits designs are shown below.

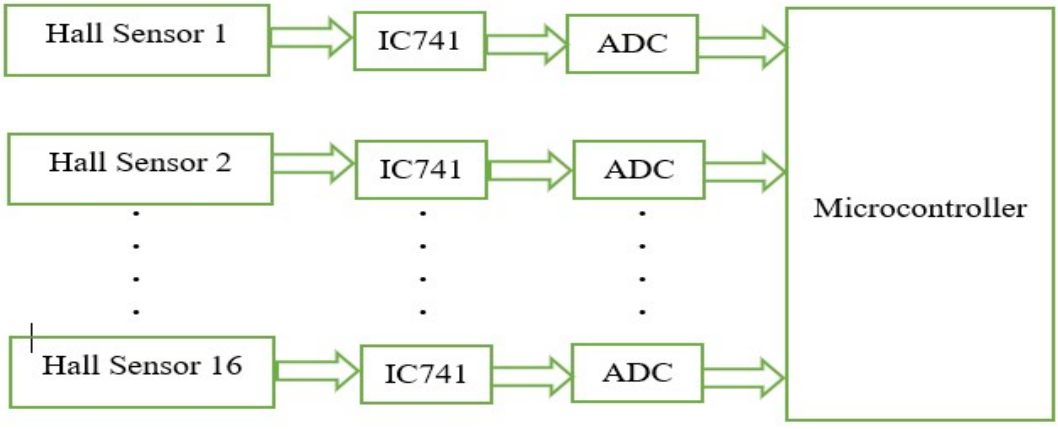

Fig.3.3 Amplifier & Buffer Stage (Design Consideration 1)

The advantages of Design 1 are:

1. Easy to implement.
2. Single stage processing.
3. Reduced signal attenuation.

The disadvantages of Design 1 are:

1. Occupies more space.
2. Larger number of ADCs.

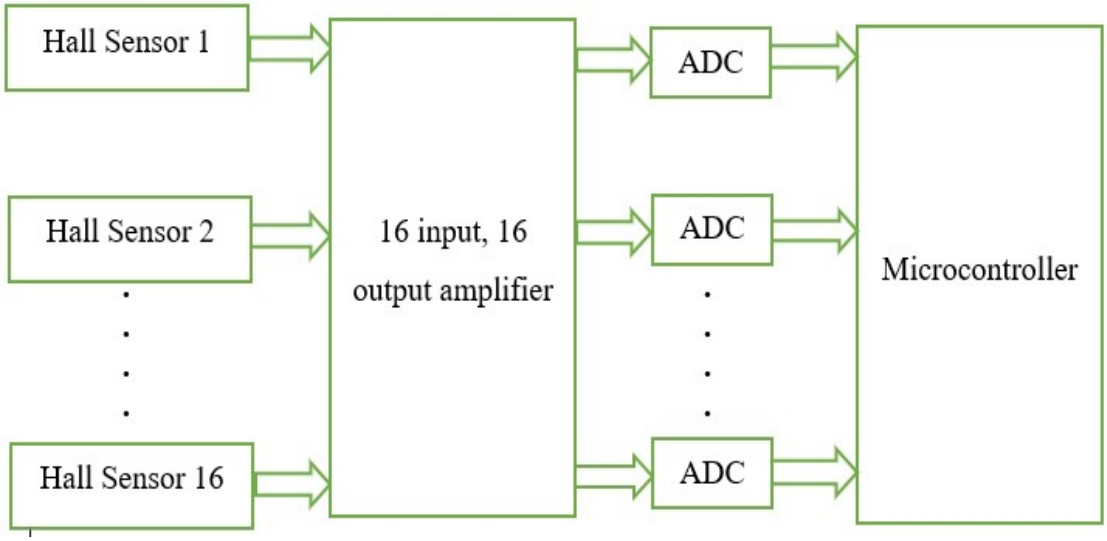

Fig.3.4 Amplifier & Buffer Stage (Design Consideration 2)

The advantage of Design 2 is that it is simpler in implementation than Design 1.

The disadvantage of this design is that it utilized unusually higher number of ADCs.

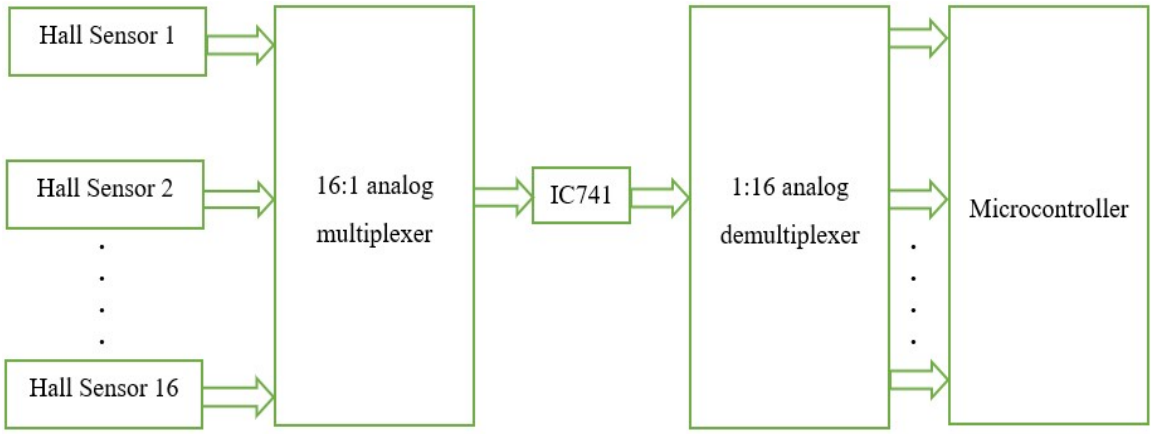

Fig.3.5 Amplifier & Buffer Stage (Design Consideration 3)

The advantages of Design 3 are:

1. Practical design.
2. Saves space, compact.

The disadvantages of Design 3 are:

1. Time delay in data acquisition.
2. Circuit complexity.

Design 3 is chosen and a few changes were made in the design as it was practically implemented. Instead of using a microcontroller, the Arduino Uno board with built in ADC of 12 bits was used. The circuit with 16 voltage inputs, 16:1 analog multiplexer (IC4067) and IC741 was simulated on Proteus but a voltage drop was observed at the output of the op-amp IC741. In order to correct this, a buffer amplifier (gain=1) was required. A buffer is used to transfer a voltage from a circuit having high output impedance level to a circuit having low impedance level. Hence, the buffer stage was designed as follows.The gain is to be 1 or close to 1 as the circuit was meant to have a unity gain output. The design will be for a non-inverting unity gain amplifier.

Therefore, gain = $1 + (R_f / R)$

$= 1 + (100 / 10000)$

$= 101 / 100 = 1.01$

Hence, the problem of voltage drop at the final output was solved using buffer amplifier.

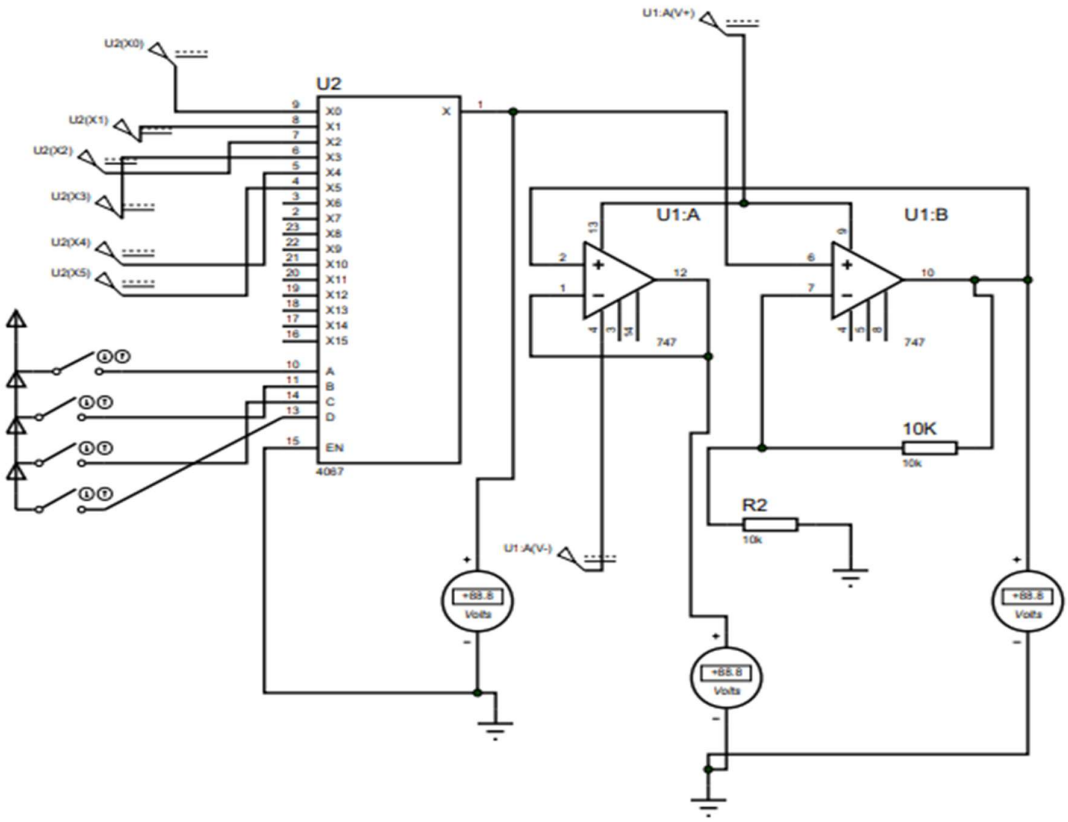

Fig.3.6 Proteus simulation of amplifier & buffer circuit

A single IC of LM747, which has two packages of Op-amp was used. And as mentioned before, an Arduino Uno board replaced the microcontroller and ADC to be used. Hence the design in Fig.3.5 was modified into the final system block diagram shown in Fig.3.7.

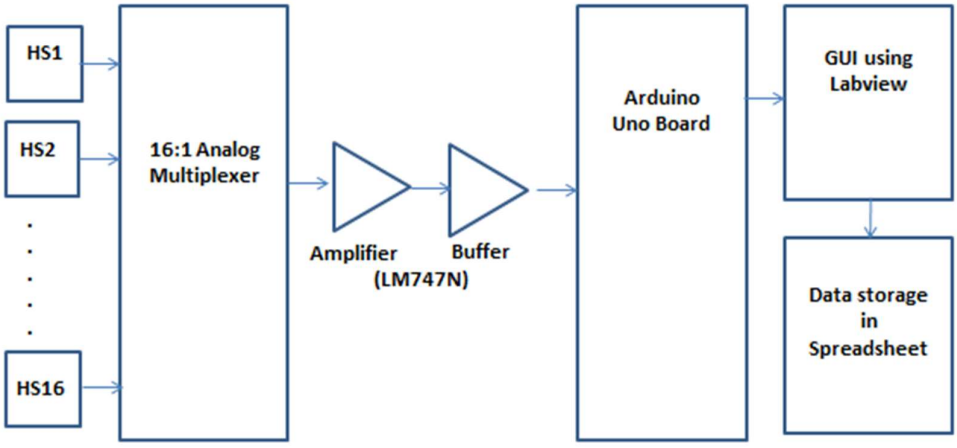

Fig.3.7 Block diagram of magnetic field measurement system

3.4 PCB Fabrication

After the initial design was complete, the process of PCB design and fabrication was started. Two schematics were created: one for the Hall sensor array and the other for the amplifier circuit. In the PCB schematic of the amplifier circuit, the value of the R_f and R resistors was changed into smaller resistor values of 10Ω and 220Ω respectively. Thus, the gain was 1.045. The PCB schematics were created on OrCAD software.

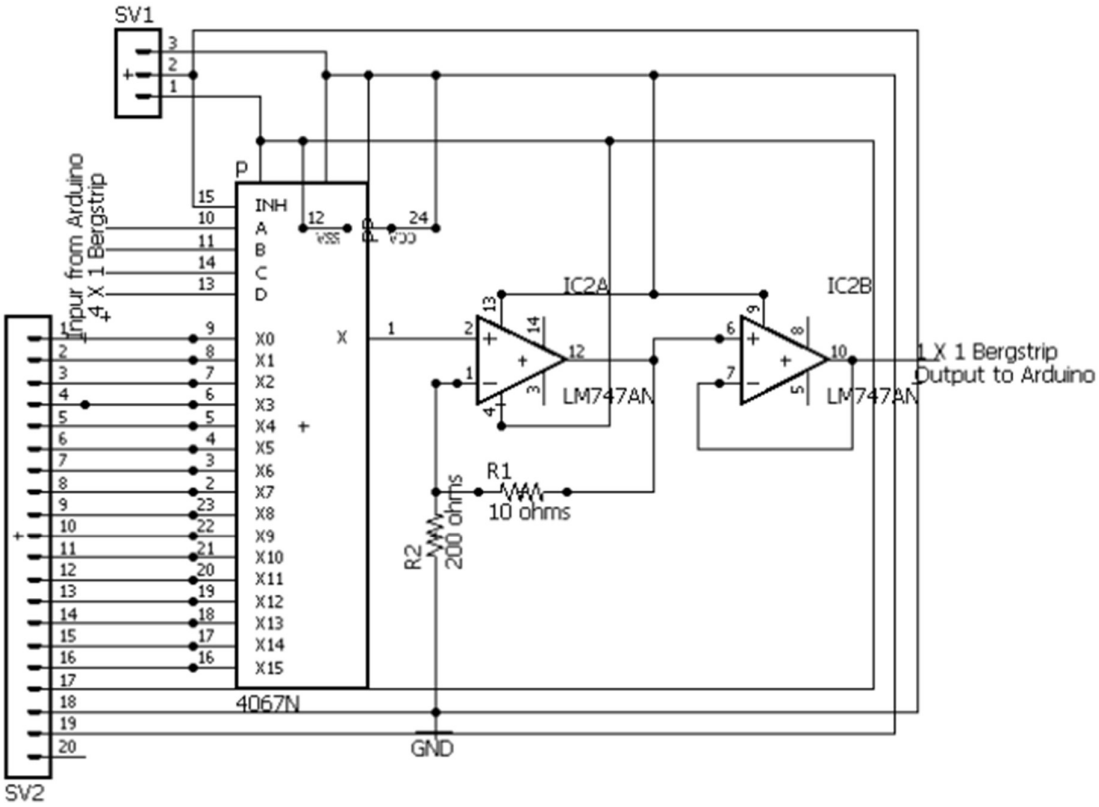

Fig.3.8 Schematic of multiplexer-amplfier-buffer module.

A double sided board design was decided upon to make the board more compact and to to allow for more routing traces on the PCB. Double sided boards are the most commonly used in the industry.

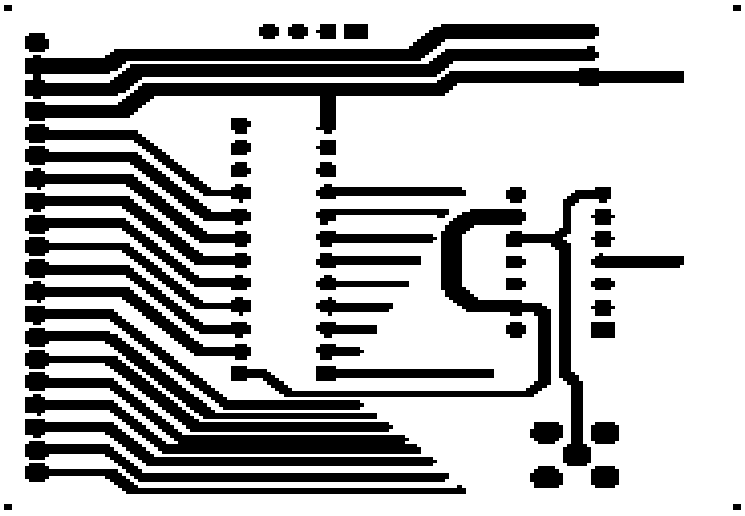

Fig.3.9 Layout of top layer of amplifier buffer module

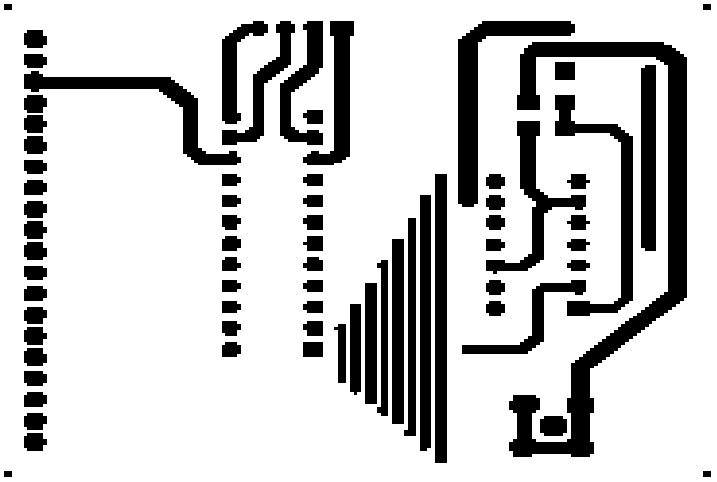

Fig.3.10 Layout of bottom layer of amplifier buffer module

For the 16 connections from the Hall probe outputs and the 3 power supply lines a flat ribbon cable connector was used. The connector used for the 16 output lines was a FCC (Flat ribbon cable connector). For the 3 power supply lines, a LEMO connector was used.
The initial design was for a 1m long PCB board for the Hall sensor array as shown in Fig.3.2, but as this design turned out to be extremely hard to implement, it was changed to individual PCB boards for each Hall sensor that would be connected by the flat ribbon cable.

Fig.3.11 Basic layout of Hall sensor mounted on PCB

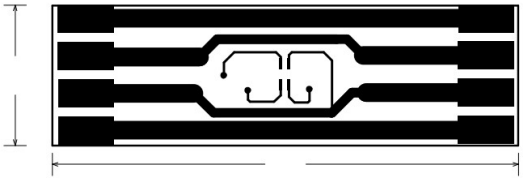

Fig.3.12 Layout for Hall sensor PCB as designed using OrCAD

The PCBs were fabricated and the type of boards used varied for the two layouts. For the Hall sensor PCB, the type of board was the thinner type, of thickness 0.8mm, as the board was to fit between the gaps of 3mm. The amplifier circuit sits outside the system and hence a thicker, more rigid board of thickness 1.6mm was used.

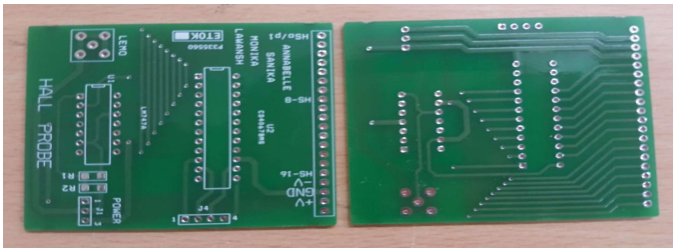

Fig.3.13 Fabricated PCB board

Fig.3.14 Board with soldered components

The Hall sensor boards were mounted on a mylar sheet and the flat ribbon cable was used to connect each of the boards in cascade and to the amplifier-buffer circuit.

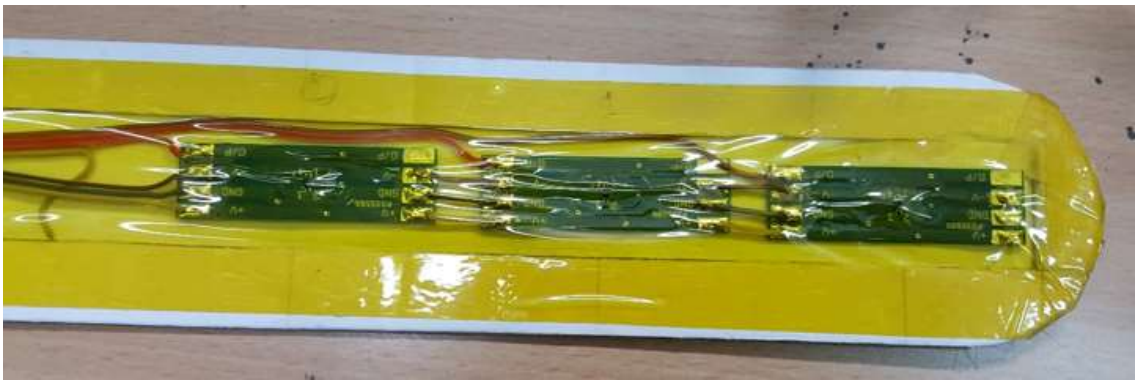

Fig.3.15 Final implementation of Hall sensor array

3.5 Software implementation

For the front panel displayed on a computer, the software used was LabVIEW. The Arduino Uno board was to be interfaced via serial communication to the LabVIEW software. Data can be stored in an Excel sheet by exporting the values from the front panel. The VISA resource name lets us select the port in which the Arduino board is connected

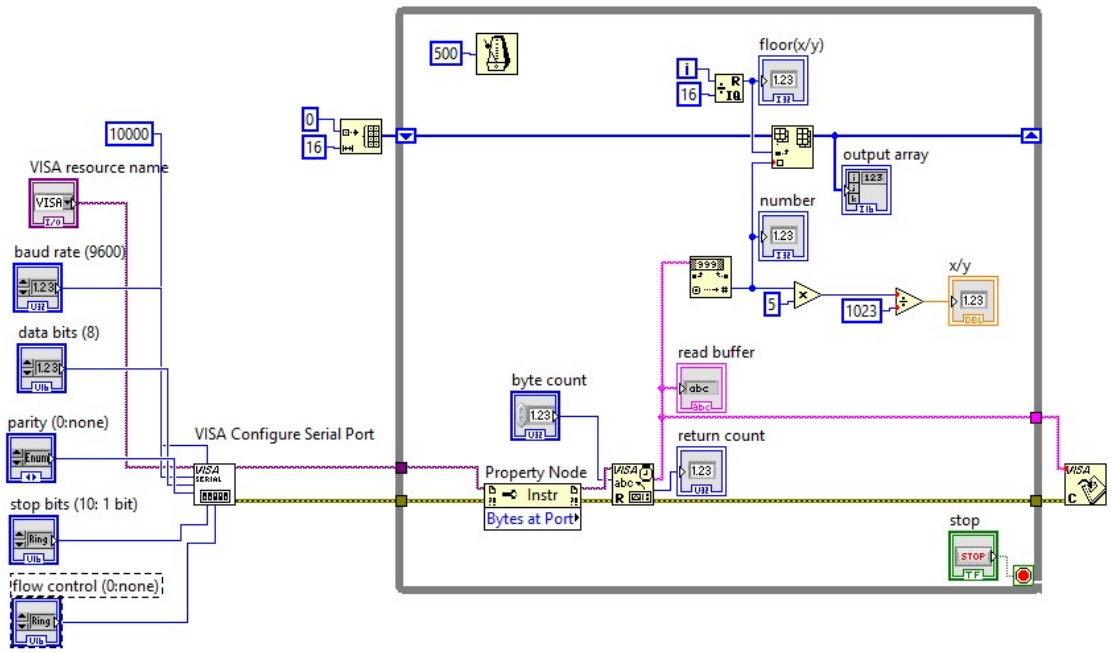

Fig.3.16 LabVIEW block diagram

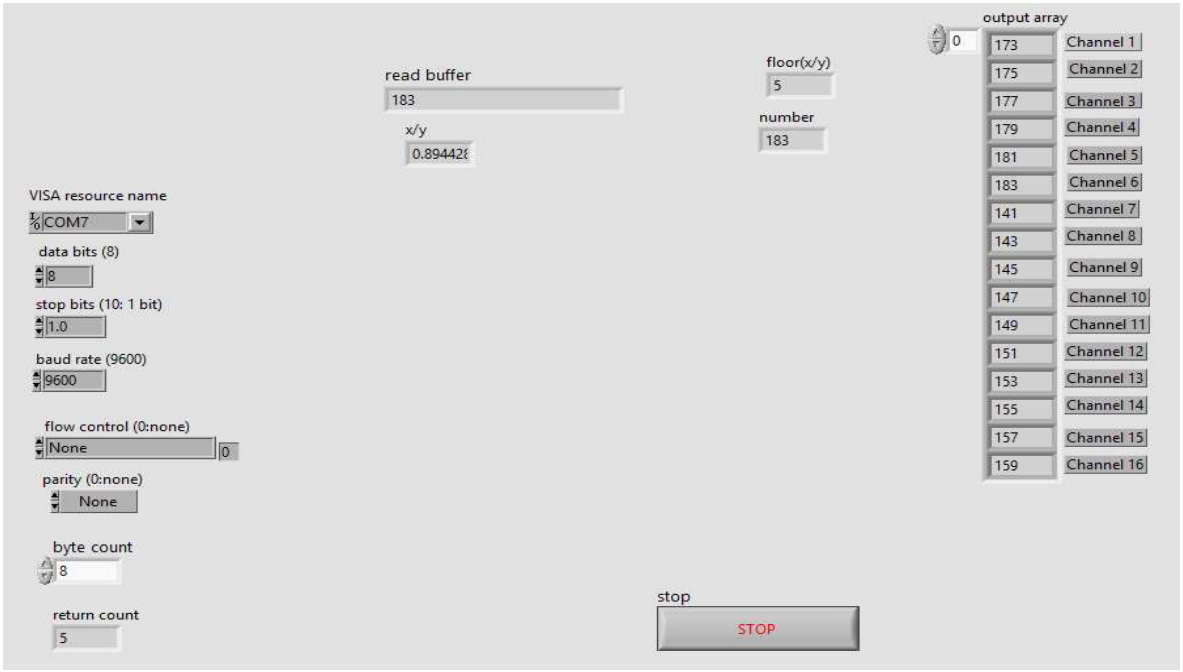

Fig.3.17 LabVIEW Front Panel (Design 1)

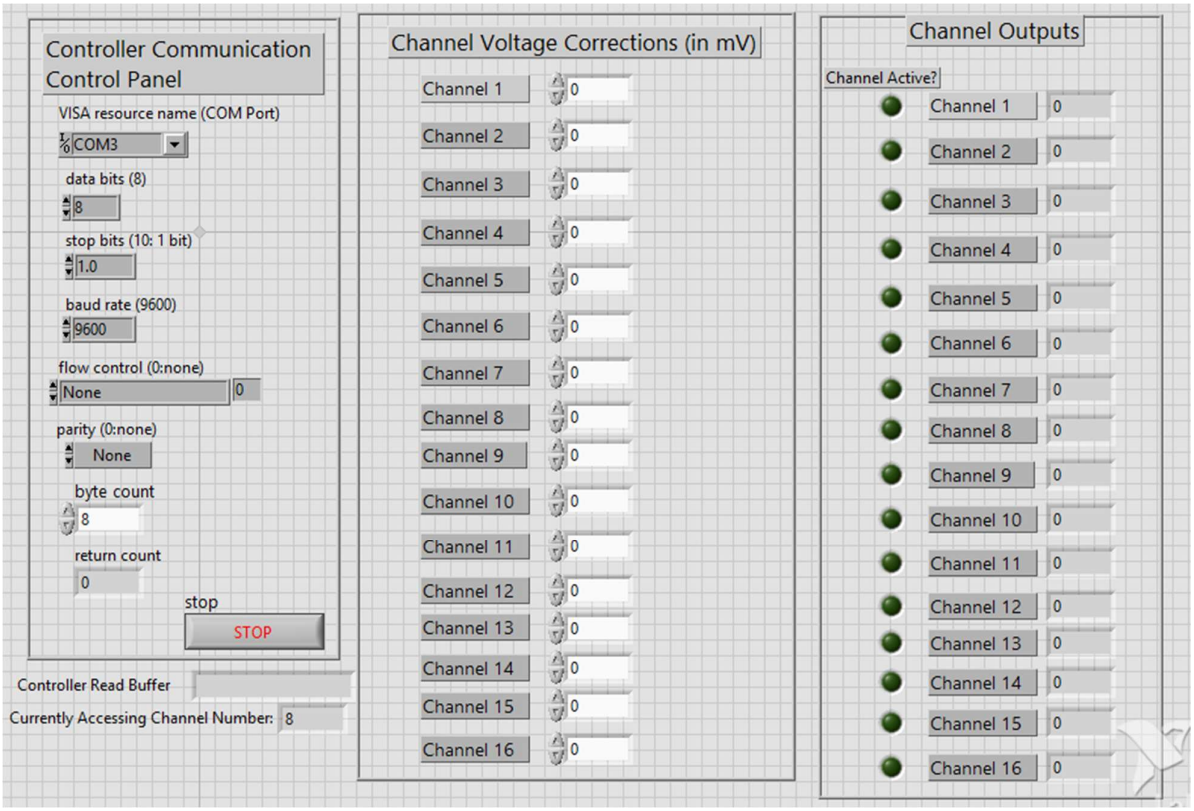

Fig.3.18 LabVIEW Front Panel (Design 2)

Chapter 4

RESULTS AND DISCUSSIONS

The results of hardware and analysis are explained in this chapter.

One of the very first tasks was to select the final sensor type before proceeding with the probe. Out of the 5 sensors initially, 2 were shortlisted out of which one had to be finalized for the probe. The testing of the hall sensor and the probe had to be done in 4 stages. Therefore, 3 tests needed to be done, each with a proper conclusion. In addition to these 3 tests, a simulation had to be carried out to ensure that the following tests. The 3 tests are listed below

1. Test 1 had to be carried as a part of qualitative analysis of the hall sensor, in which the sensor is kept between two permanent magnets and the separation between the magnets was varied, which in turn varied the magnetic field. Also, one of the two types of sensor was finalized depending upon this test.

2. Test 2 was carried out as a part of reproducibility test to check if same data was obtained for same conditions in two iterations.

3. Test 3 was done as a part of relative calibration to check linear regression of the hall sensor array

4.1 Test 1: Qualitative Analysis

In this test, a single hall sensor was mounted on a matrix type PCB and power and output connections were made. This PCB was placed between two permanent magnets and the distance between these magnets was varied manually as shown in fig 4.1

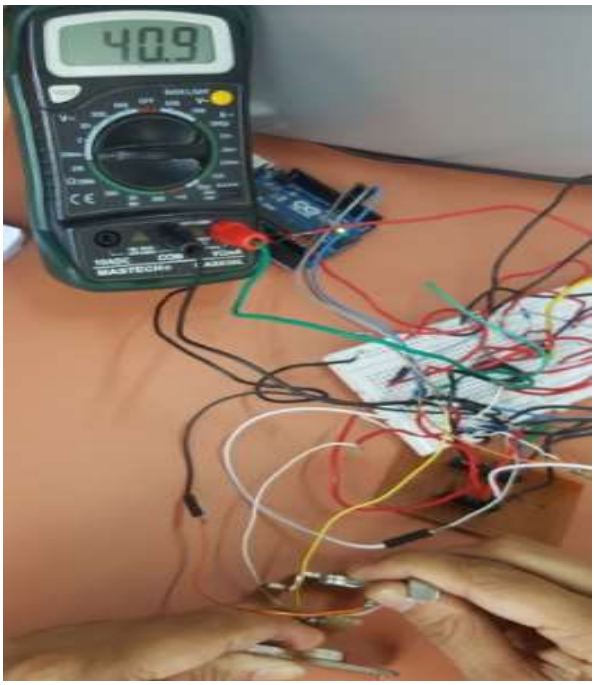

Fig.4.1 Test 1 using permanent Magnets

Fig.4.2 Hall IC on Matrix PCB

To increase magnetic field further, another pair of magnets were also added. As the distance between two magnets was reduced, magnetic field increased. This was reflected in the hall voltage which was obtained from the sensor. Hall voltages were plotted by varying this distance and a curve was obtained From Fig 4.2 it can be verified that magnetic field increased with decrease in separation between magnets, which was reflected by the hall voltage obtained. Higher the magnetic field, higher the hall voltage obtained.

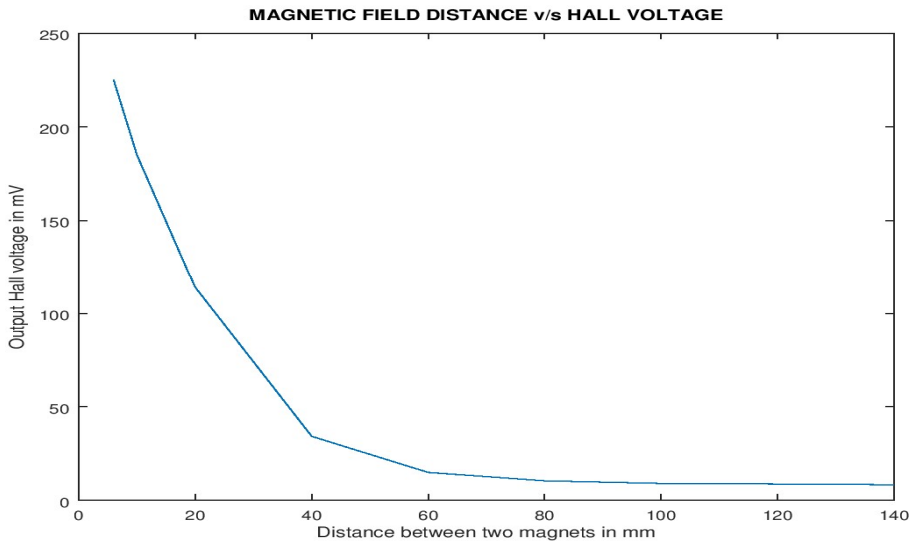

Fig.4.3 Qualitative testing of the system using a pair of permanent magnets

Also, in one of the tests, both types of sensors (CYSJ106C and CYSJ166A) were kept together between the magnets and readings were obtained as shown in the table 4.1

Table.4.1 Comparative performance study of two of the Hall sensors

Sr. No.	Measuring Conditions	Output Voltages (in mV)
1	One pair of magnets	CYSJ106C: 40.9
2	Two pairs of magnets	CYSJ106C: 116.3
3	One pair of magnets with two hall sensors kept side by side	CYSJ106C: 31.1 CYSJ166A: 41.6

4.2 Test 2: Reproducibility Tests

For faithful operation of any system, same readings should be obtained for same operating conditions. Therefore, reproducibility tests were done by measuring values of magnetic field at two different instances. The results obtained are shown in Table 4.1. Some channels were selected at random and the corresponding hall sensor readings were taken without placing any magnetic field source. Afterwards, the corresponding sensor was placed between two magnets and the readings were obtained. This exercise was repeated twice and the results obtained in both the iterations matched, indicating faithful operation of the system.

Table.4.2 Test results of reproducibility studies of the Hall sensor array.

Channel No.	Reading 1 (in mV)		Reading 2 (in mV)	
	Without Magnets	With Magnets	Without Magnets	With Magnets
2	120	660	120	660
4	210	620	210	640
6	160	700	170	700
8	210	660	210	680
10	120	600	120	620
12	170	560	180	540

4.3 Test 3: Calibration (Relative and Absolute)

In order to convert hall voltage into equivalent magnetic field, calibration was needed. This included measuring hall voltages for known values of magnetic field, plotting hall voltage v/s magnetic field graph and measuring the slope and offset of the curve. This slope will give us the multiplication factor for Volt to Tesla conversion as shown in fig. 4.4. This testing was carried out with the help of ECR ion source machine, wherein the field was controlled via control room with the help of Labview. The field was increased in steps of 200 Gauss.

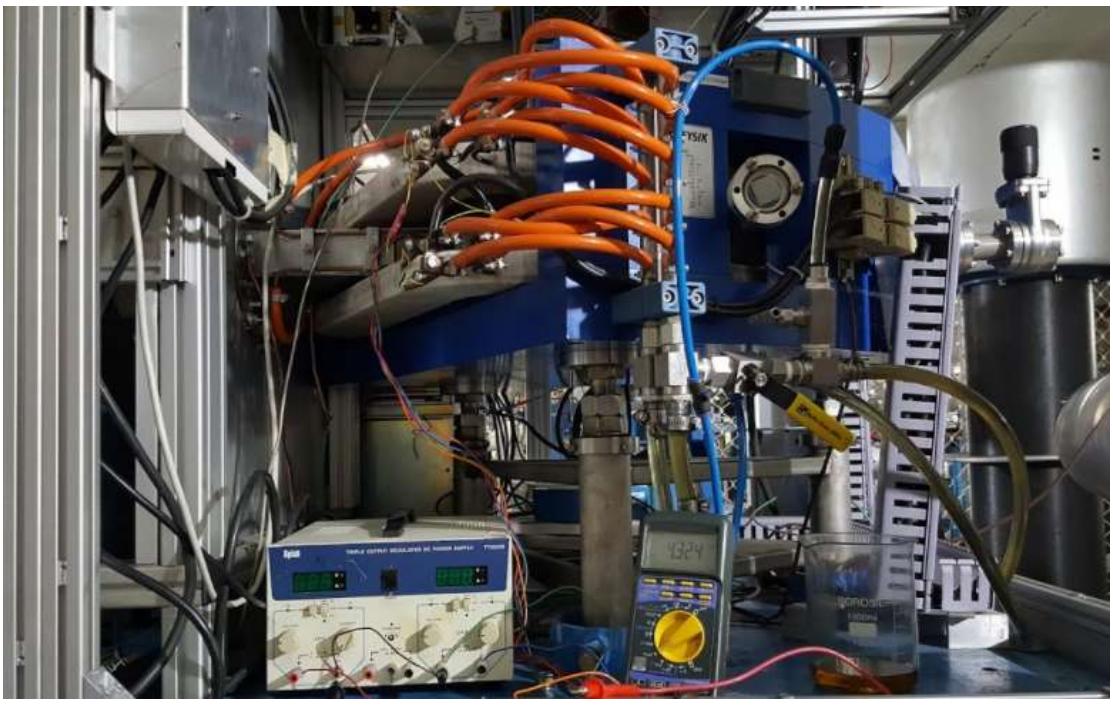

Fig4.4 Testing under ECR Ion Source

The corresponding Sensor reading was measured. The temperature in the laboratory was 20 degree Celsius. The overall pictorial view of the setup can be seen from fig.4.4. The sensor was placed between 90◦ bending dipole magnet at mid position as seen in the fig.4.5. The maximum field that can be achieved in this magnet is 0.3T

Fig.4.5 Hall Sensor position

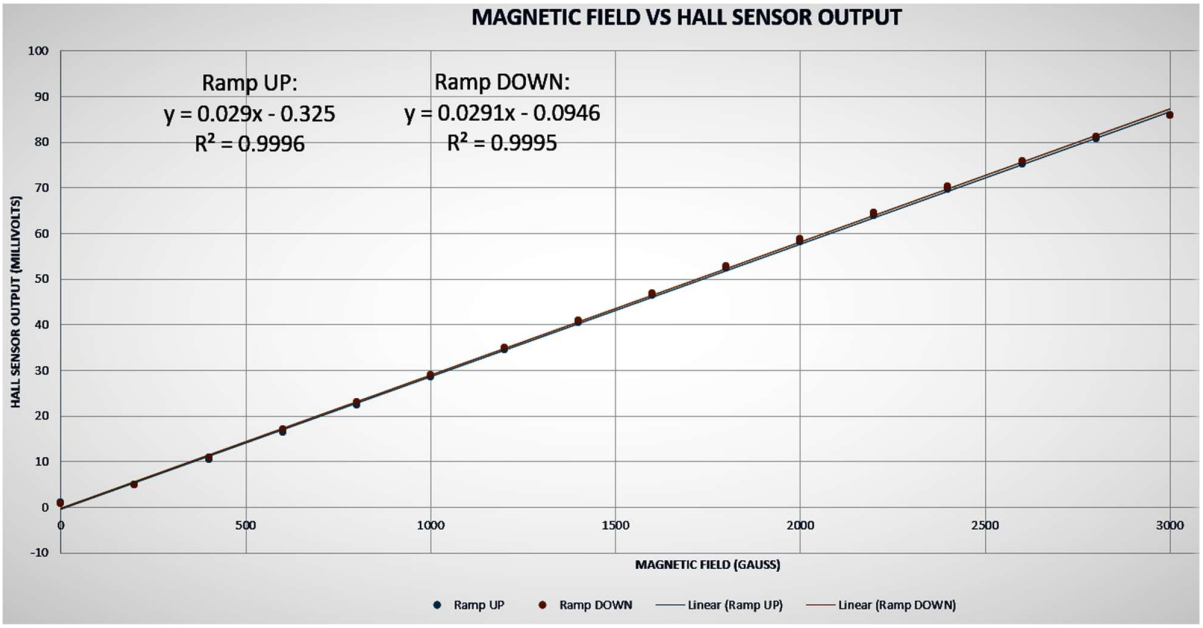

Fig.4.6 Magnetic Field v/s Output Voltage plot

Relative calibration was performed in which the hall voltage v/s magnetic field curve showed a regression of 0.9996 during ramp up and 0.9995 during ramp down operations. The regression shows how accurately the obtained curve fits onto a linear curve, where a regression of 1 is highly desirable. Fig4.6 shows the relative calibration curve

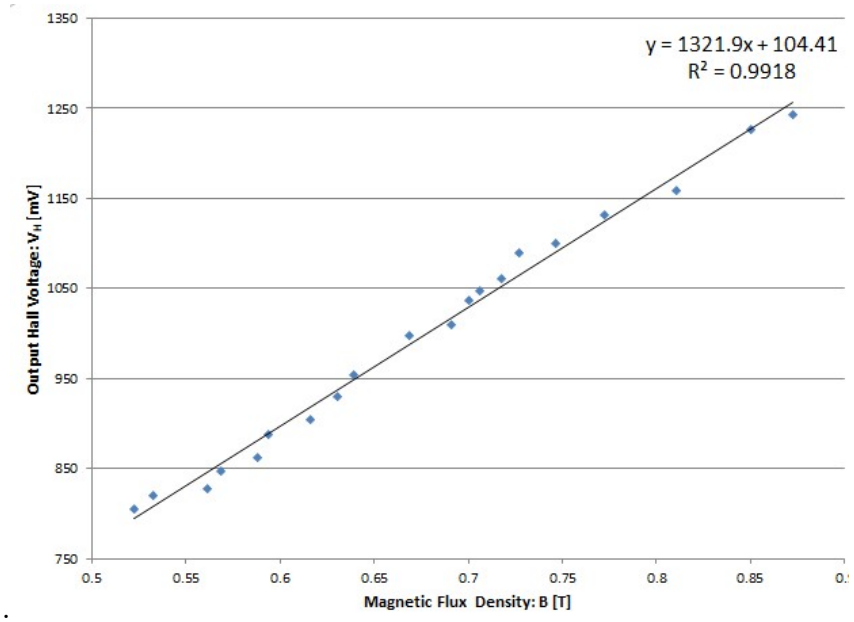

Fig.4.7 Absolute Calibration Graph

Figure 4.7 shows the absolute calibration of the system, wherein voltage readings were captured by varying magnetic field of a strong permanent magnet as seen in the figure below. The permanent magnet has four screws at the top which can be used to vary the distance between the two poles of the magnet. A commercial hall probe was used to cross check the sensor board readings. The commercial hall probe readings and sensor readings were taken simultaneously at each step by varying the field. The supply voltage was kept at 6V. The digital teslameter with the commercial hall probe attached to it can measure field strength up to 3T. The offset of the sensor board obtained was almost constant around 1.5 mV.

From the equation of the above curve, it can be observed that the slope of the graph is 1321.9 mV/T. The inverse of this value is to be multiplied to the voltage readings obtained to get the required magnetic field. The regression of the curve is 0.9918, which an indicator of the agreement of the values with linear trend.

Fig.4.8 Absolute Calibration Testing

The graph shown in the figure 4.7 was plotted based on Table no.4.3, which is shown below.

Table.4.3 Absolute calibration readings.

Magnetic Field (in Tesla)	Voltage Readings (in mV)
0.87225	1243
0.84995	1227
0.8105	1158.5
0.77205	1131.3
0.74605	1100.1
0.7264	1089.8
0.7179	1061.1
0.70605	1048.3
0.7002	1036.9
0.6905	1010.6
0.6682	998
0.63915	955.1
0.6303	930.3
0.6155	905.2
0.5936	887.5
0.58805	863
0.5685	846.9
0.56065	829.1
0.5327	820.3
0.52205	805.6
0.87225	1243

4.4 Precision Calculations of the System

The precision stated in the requirement sheet was 0.2% of full scale reading

Full scale reading for the probe = 30,000 Gauss

0.2% of Full Scale = $\frac{0.2}{100} \times 30000 = 60$ Gauss .

Therefore, desired Precision is 60 Gauss. From the datasheets, it is known that Hall Voltage varies from 110 mV to 150 mV at 100 mT So, two calculations must be done- worst case and best case precision

Worst Case:-

Hall Voltage at 100 mT (or 1000 G) = 110 mV

Sensitivity (Gauss/mV) = $\frac{1000}{110}$ = 9.09 G/mV

ADC resolution = 10 bit or 1024 quantization levels

Dynamic range of ADC = 0 to 5 V .

Hence, Least Count (or Step Size) of ADC = $\frac{5}{1024} \approx$ 5 mV

Therefore, Worst Case Least Count of Probe = 9.09 × 5 = **45.45 G**

Best Case:-

Hall Voltage at 100 mT (or 1000 G) = 150 mV

Sensitivity (Gauss/mV) = $\frac{1000}{150}$ = 6.66 G/mV

ADC resolution = 10 bit or 1024 quantization levels

Dynamic range of ADC = 0 to 5 V

Hence, Least Count (or Step Size) of ADC = $\frac{5}{1024} \approx$ 5 mV

Therefore, Best Case Least Count of Probe = 6.66 × 5 = **33.33 G**

The above calculations show that both best case and worst case precision calculations lie well within the range of 0 to 60 Gauss

Also, precision can be improved by compromising full scale measurements as follows-

Case 1:- Let Maximum Magnetic field to be measured = 30,000 Gauss (3 Tesla)

Let sensitivity be 6.66 G/mV (Best case precision calculation)

Hall voltage at 30,000 G = $\frac{30000}{6.66 \times 100} = 4.5$ V

Dynamic Range of ADC = 0 to 5 V

Let gain of amplifier = 1

Therefore, Least count of magnetic field = 33.33 G

Case 2:- Let Maximum Magnetic field to be measured = 15,000 Gauss (1.5 Tesla)

Let sensitivity be 6.66 G/mV (Best case precision calculation)

Hall voltage at 15,000 G = $\frac{15000}{6.66 \times 100} = 2.25$ V

Dynamic Range of ADC = 0 to 5 V

Let gain of amplifier = 2

Therefore, Least count of magnetic field = 16.65 G

From the calculations shown above, following conclusions can be drawn-

1. Higher precision can be achieved at the cost of reduced dynamic range.
2. ADC with a higher resolution can be used, but the chances of data corruption due to noise also increases

Chapter 5

SUMMARY AND CONCLUSION

5.1 Summary

The project envisages making a Hall sensor array based magnetic measurement system to be used for the Iron Calorimeter (ICAL) detector of the INO project. An extensive literature survey was carried out to find out the existing techniques and systems which are used to measure magnetic fields and why they are not suitable for our particular application. The literature survey also included the study of magnetic fields and Hall sensors which are most suitable for our specific application. Design of the circuit and system, taking the electric and mechanical parameters and constraints into consideration was the next step. The probe that we designed is capable of measuring strong magnetic fields (of up to 1.5T) produced within the ICAL magnet using the Hall sensors. The sensed signals are then multiplexed, amplified, buffered and given to the inbuilt 12-bit ADC of the Arduino Uno board. The Arduino Board is interfaced with LabVIEW using serial communication bus. The digital data is displayed on the front panel screen of the LabVIEW software and can be exported and stored in an Excel sheet for future analysis.

5.2 Conclusion

The amplifier and buffer circuitry was initially tested using voltage inputs instead of actual signals produced by the magnetic fields to ensure that this stage was operating smoothly. Later on, the system was checked by using both the CYSJ106C & CYSJ166A Hall sensor ICs. After

extensive tests and studies, we concluded that the CYSJ106C sensor was better suited for our requirements. After the PCBs were designed and fabricated, further tests were carried out using the ECR Ion Accelerator (Electron Cyclotron Resonance based Ion Accelerator) available at TIFR, Mumbai. The data showed excellent linearity in reference to the ECR measurement system. However, the obtained values were found to be lower than the expected value as per its data sheet. This was due to the fact that the Hall sensor assembly could not be placed exactly at the center of the magnet (due to some access constraints) from which point the measurements were taken by the ECR accelerator system. We then conducted some detailed absolute calibration studies by using a strong permanent magnet whose field could be varied by the changing the distance between the two poles. The readings obtained by our Hall sensors were compared with those from a commercial Hall probe under the same magnetic field conditions. The results were found to be satisfactory and thus we could obtain the absolute calibration of our probe.

5.3 Future Scope

The probe that we designed and developed satisfies the specifications and requirements of the INO project. The probe might be used in the actual application for measurement of ICAL detector's insitu magnetic fields next month. However, there are a number of areas that can be worked up on to improve the system and its functionality. We are currently designing an one meter long printed circuit board on which the sensors and the electronics is being integrated on the board. By building the probe on a PCB, we could also reduce thickness of the probe to about 2mm, which is one of the main requirements of the probe. The LabVIEW front-end interface will be improved to include more functionality and user friendly features which are required for the operation, data acquisition and display. The ultimate objective of this prototype system is to fine tune the system and produce a large number of boards which are needed by the INO project in Madurai.

Appendix I

I.a Introduction

At the end of the project work at stage 1 and 2 students will be able to:

C421.1 (CO-1): Apply the knowledge based on curricular and co-curricular activities to solve electronics and telecommunication based project work.

The knowledge acquired through curricular and co-curricular activities like Digital signal processing, Analog electronics, Micro-controller and its applications was applied in implementing the hardware circuits and analysis in the project.

C421.2 (CO-2): Systematically analyze electronics and telecommunication related project based on the literature review.

The extensive literature survey was carried out for various aspects of the project such as working of the Hall sensor, applications of the magnetic sensors in various fields, existing technologies to measure the strength of magnetic field, etc.

C421.3 (CO-3): Design and develop hardware circuit and/or software code based on the problem specifications about the project.

Hall probe board was being designed and implemented for testing magnetic field.

C421.4 (CO-4): Carry out different experiments to generate data, analyze and interpret the data, and draw valid conclusions related on the project work.

Multiple tests were conducted and numerous readings were taken with designed Hall probe board.

C421.5 (CO-5): Select and apply appropriate modern tools for the solution of their project problem.

Proteus, Arduino, OrCAD, and LabVIEW are the software tools used in the project .

C421.6 (CO-6): Know the responsibility of the engineer towards the society with respect to their project work.

The project is a research project for an industrial application and hence, it does not have much in terms of day-to-day applications.

C421.7 (CO-7): Understand the impact of engineering solutions related to their project work in societal context for sustainable development.

C421.8 (CO-8): Apply professional ethical principles while project implementation, report writing, and publication.

Professional and personal ethics were followed in documentation of and preparation of report. Appropriate citations and references were given as required .

C421.9 (CO-9): Work effectively as an individual and as a member of the team while the project work is carried out.

The members of the team were able to work effectively for developing individual modules in the project according to their areas of specialization. They were also able to work effectively as a team while integrating these modules together.

C421.10 (CO-10): Communicate effectively while project report writing and oral/visual presentations.

Each presentation had an improved aspect based on the discussions and feedback from the previous presentations. The report was also modified accordingly

C421.11 (CO-11): Gain knowledge of engineering and management aspects while the project is being implemented. The knowledge of various engineering and management aspects such as performance, feasibility, accuracy, cost effectiveness, etc. was gained.

Proper work and time management was done. Finance was sponsored by TIFR hence mapping is 1.

C421.12 (CO-12) Engage themselves in independent and lifelong learning.

Concepts learned while executing the project will be used for further projects and research.

I.b Mapping course outcomes with program outcomes

Table shows mapping of course outcomes with program outcomes.

(*Note: 1: Slightly 2: Moderately 3: Substantially If there is no correlation the cell to be left blank or put* **-)**

	Program Outcomes											
Course Outcomes	PO1	PO2	PO3	PO4	PO5	PO6	PO7	PO8	PO9	PO10	PO11	PO12
CO1	3	-	-	-	-	-	-	-	-	-	-	-
CO2	-	3	-	-	-	-	-	-	-	-	-	-
CO3	-	-	2	-	-	-	-	-	-	-	-	-
CO4	-	-	-	3	-	-	-	-	-	-	-	-
CO5	-	-	-	-	2	-	-	-	-	-	-	-
CO6	-	-	-	-	-	1	-	-	-	-	-	-
CO7	-	-	-	-	-	-	-	-	-	-	-	-
CO8	-	-	-	-	-	-	-	3	-	-	-	-
CO9	-	-	-	-	-	-	-	-	3	-	-	-
CO10	-	-	-	-	-	-	-	-	-	2	-	-
CO11	-	-	-	-	-	-	-	-	-	-	1	-
CO12	-	-	-	-	-	-	-	-	-	-	-	3

Appendix II

DATASHEETS

Arduino Uno Datasheet

Product Overview

The Arduino Uno is a microcontroller board based on the ATmega328 (datasheet). It has 14 digital input/output pins (of which 6 can be used as PWM outputs), 6 analog inputs, a 16 MHz crystal oscillator, a USB connection, a power jack, an ICSP header, and a reset button. It contains everything needed to support the microcontroller; simply connect it to a computer with a USB cable or power it with a AC-to-DC adapter or battery to get started. The Uno differs from all preceding boards in that it does not use the FTDI USB-to-serial driver chip. Instead, it features the Atmega8U2 programmed as a USB-to-serial converter.

"Uno" means one in Italian and is named to mark the upcoming release of Arduino 1.0. The Uno and version 1.0 will be the reference versions of Arduno, moving forward. The Uno is the latest in a series of USB Arduino boards, and the reference model for the Arduino platform; for a comparison with previous versions, see the index of Arduino boards.

Technical Specification

EAGLE files: arduino-duemilanove-uno-design.zip Schematic: arduino-uno-schematic.pdf

Summary

Microcontroller	ATmega328
Operating Voltage	5V
Input Voltage (recommended)	7-12V
Input Voltage (limits)	6-20V
Digital I/O Pins	14 (of which 6 provide PWM output)
Analog Input Pins	6
DC Current per I/O Pin	40 mA
DC Current for 3.3V Pin	50 mA
Flash Memory	32 KB of which 0.5 KB used by bootloader
SRAM	2 KB
EEPROM	1 KB
Clock Speed	16 MHz

the board

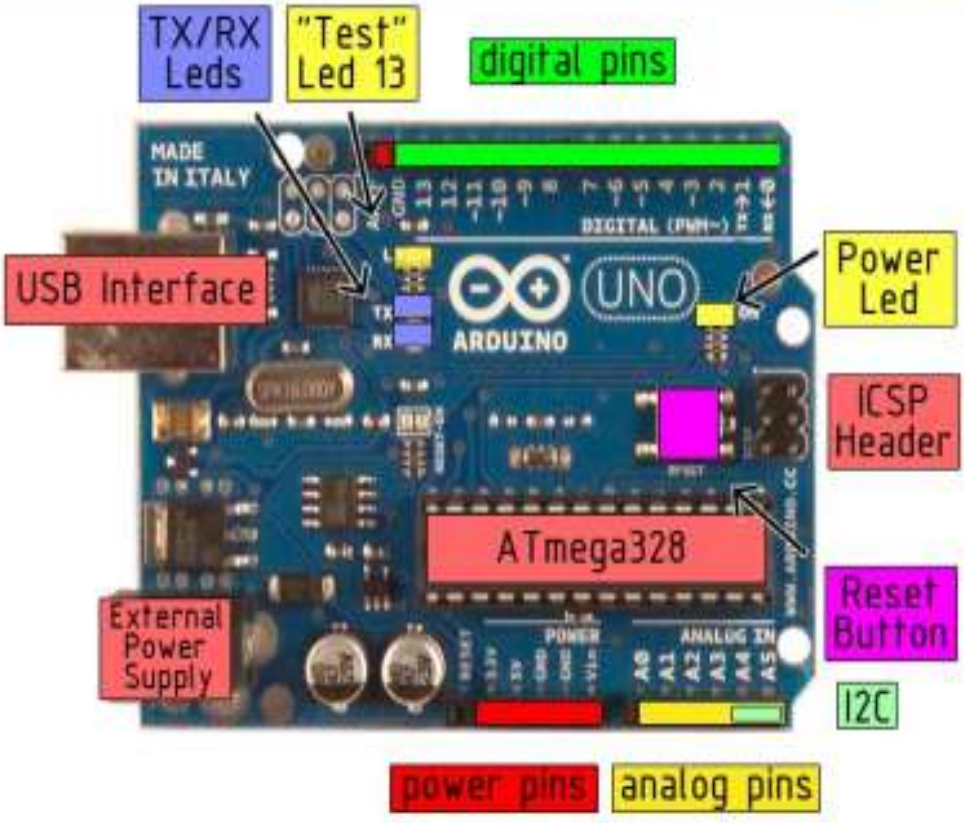

Power

The Arduino Uno can be powered via the USB connection or with an external power supply. The power source is selected automatically.

External (non-USB) power can come either from an AC-to-DC adapter (wall-wart) or battery. The adapter can be connected by plugging a 2.1mm center-positive plug into the board's power jack. Leads from a battery can be inserted in the Gnd and Vin pin headers of the POWER connector.

The board can operate on an external supply of 6 to 20 volts. If supplied with less than 7V, however, the 5V pin may supply less than five volts and the board may be unstable. If using more than 12V, the voltage regulator may overheat and damage the board. The recommended range is 7 to 12 volts.

The power pins are as follows:

- **VIN.** The input voltage to the Arduino board when it's using an external power source (as opposed to 5 volts from the USB connection or other regulated power source). You can supply voltage through this pin, or, if supplying voltage via the power jack, access it through this pin.
- **5V.** The regulated power supply used to power the microcontroller and other components on the board. This can come either from VIN via an on-board regulator, or be supplied by USB or another regulated 5V supply.
- **3V3.** A 3.3 volt supply generated by the on-board regulator. Maximum current draw is 50 mA.
- **GND.** Ground pins.

Memory

The Atmega328 has 32 KB of flash memory for storing code (of which 0,5 KB is used for the bootloader); It has also 2 KB of SRAM and 1 KB of EEPROM (which can be read and written with the EEPROM library).

Input and Output

Each of the 14 digital pins on the Uno can be used as an input or output, using pinMode(), digitalWrite(), and digitalRead() functions. They operate at 5 volts. Each pin can provide or receive a maximum of 40 mA and has an internal pull-up resistor (disconnected by default) of 20-50 kOhms. In addition, some pins have specialized functions:

- **Serial: 0 (RX) and 1 (TX).** Used to receive (RX) and transmit (TX) TTL serial data. TThese pins are connected to the corresponding pins of the ATmega8U2 USB-to-TTL Serial chip .
- **External Interrupts: 2 and 3.** These pins can be configured to trigger an interrupt on a low value, a rising or falling edge, or a change in value. See the attachInterrupt() function for details.
- **PWM: 3, 5, 6, 9, 10, and 11.** Provide 8-bit PWM output with the analogWrite() function.
- **SPI: 10 (SS), 11 (MOSI), 12 (MISO), 13 (SCK).** These pins support SPI communication, which, although provided by the underlying hardware, is not currently included in the Arduino language.

- **LED: 13.** There is a built-in LED connected to digital pin 13. When the pin is HIGH value, the LED is on, when the pin is LOW, it's off.

CYSJ106C Datasheet

Version 2
Released in May 2016
Dr.-Ing. habil. Jigou Liu

Chen Yang Technologies GmbH & Co. KG

CYSJ106C GaAs HALL-EFFECT ELEMENTS

CYSJ106C series Hall-effect element is a ion-implanted magnetic field sensor made of mono-crystal gallium arsenide (GaAs) semiconductor material group III-V using ion-implanted technology. It can convert a magnetic flux density signal linearly into voltage output.

FEATURES

- High Linearity
- Superior Temperature Stability
- Miniature Package
- Wide measuring range 0-3T

TYPICAL APPLICATION

- Magnetic Field Measurement
- DC Brushless Motor
- Current Sensor
- Non-contact Switch
- Position Control
- Detection Of Revolution

BLOCK DIAGRAM

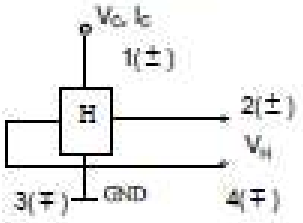

ABSOLUTE MAXIMUM RATING

Parameter	Symbol	Value	Unit
Max. Input Current/Voltage	I_C/V_C	13mA/ 10V	mA/V
Max. Input Power	P_D	150	mW
Operating temperature range	T_A	-40~125	°C
Storage temperature range	T_S	-55~150	°C

ELECTRICAL CHARACTERISTICS（T_A=25°C）

Parameter	Symbol	Test conditions	Value	Unit
Hall output voltage	V_H	B=100mT, I_C=8mA/V_C=6V	110~150	mV
Offset voltage	Vos(Vu)	V_C=6V, B=0mT	±11	mV
Input resistance	R_{in}	B=0mT, I_C=0.1mA	650~850	Ω
Output resistance	R_{out}	B=0mT, I_C=0.1mA	650~850	Ω
Temperature coefficient of Hall output voltage	αV_H	I_C=5mA, B=100mT (Ta=25°C ~ 125°C)	-0.06	%/°C
Temperature coefficient of input and output resistance	αR_{in} αR_{out}	I_C=0.1mA, B=0mT (Ta=25°C ~ 125°C)	0.3	%/°C
Linearity	ΔK_H	I_C=5mA B=0.1/0.5T	2	%

Notes:

$$\alpha V_H = \frac{1}{V_H(T_1)} x \frac{V_H(T_2)-V_H(T_1)}{T_2-T_1} x100.$$

$$\alpha R_{in} = \frac{1}{R_{in}(T_1)} x \frac{R_{in}(T_2)-R_{in}(T_1)}{T_2-T_1} x100$$

$$\Delta K_H = \frac{K(B_1)-K(B_2)}{[K(B_1)+K(B_2)]} x200$$

$$K_H = \frac{V_H}{I_C B}$$

T_1=25°C, T_2=125°C, B_1=0.5T, B_2=0.1T

Markt Schwabener Str. 8
D-85464 Finsing
Germany

Tel.: +49 (0)8121 – 2574100
Fax: +49 (0)8121 – 2574101
Email: info@cy-sensors.com
http://www.cy-sensors.com

Package Outline Drawing (Unit: mm)

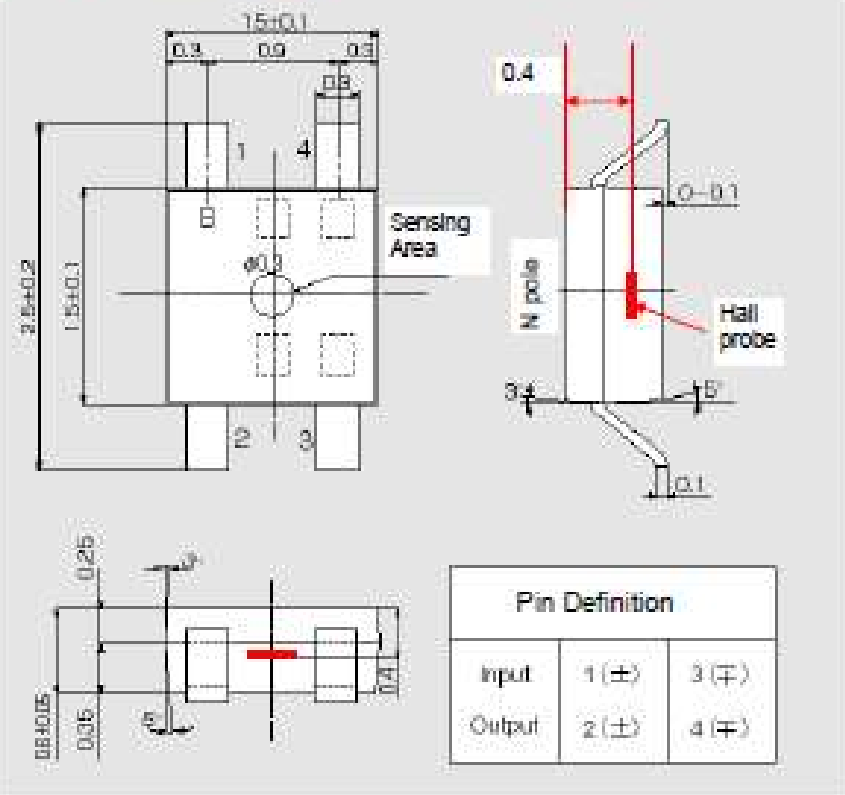

Pin Definition		
Input	1 (±)	3 (∓)
Output	2 (±)	4 (∓)

Characteristic Curves

Allowable Package Power Dissipation

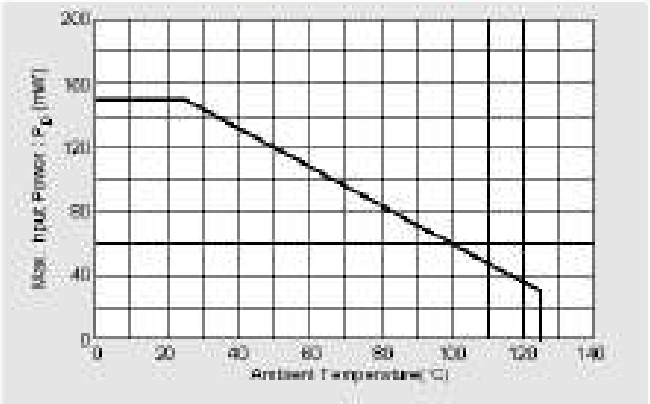

Markt Schwabener Str. 8
D-85464 Finsing
Germany

Tel.: +49 (0)8121 – 2574100
Fax: +49 (0)8121– 2574101
Email: info@cy-sensors.com
http://www.cy-sensors.com

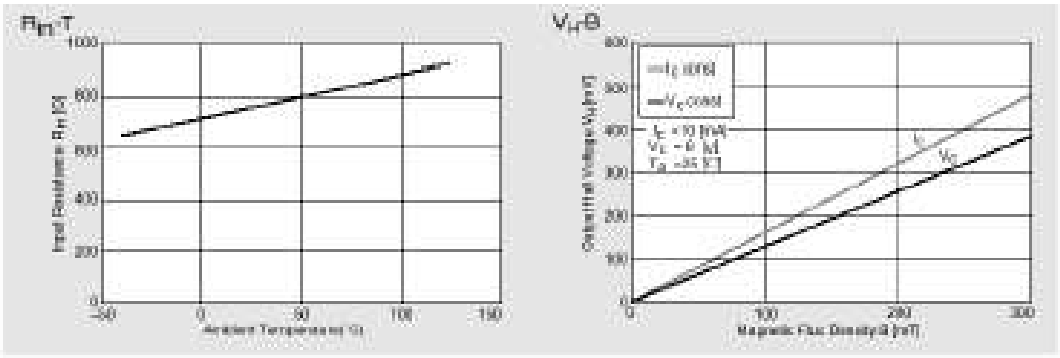

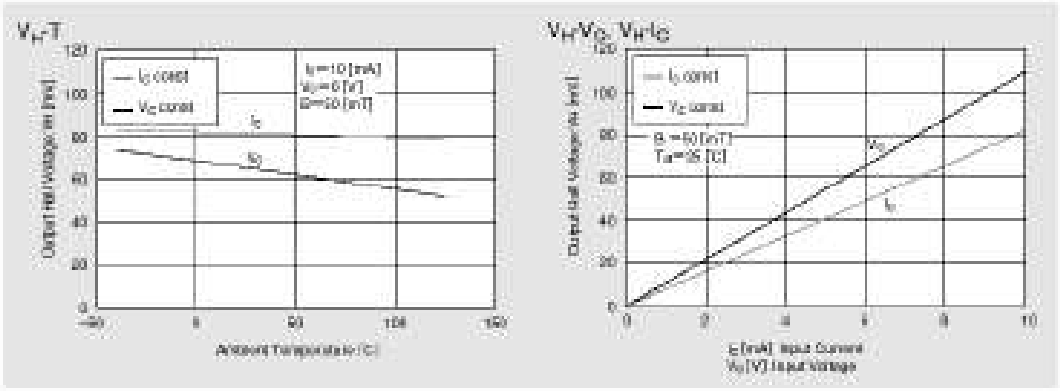

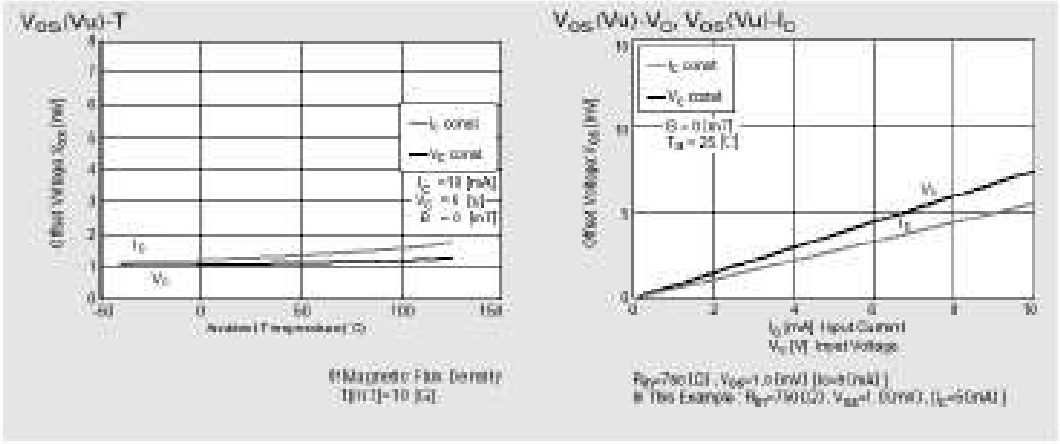

Markt Schwabener Str. 8
D-85464 Finsing
Germany

Tel.: +49 (0)8121 – 2574100
Fax: +49 (0)8121– 2574101
Email: info@cy-sensors.com
http://www.cy-sensors.com

Connection

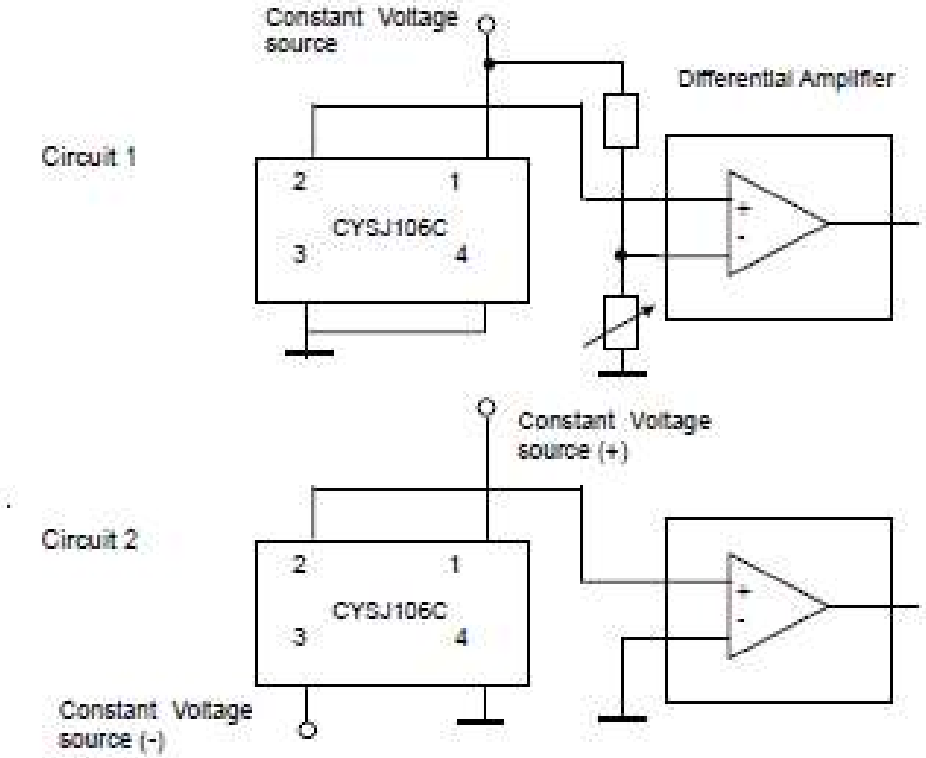

Application Notes

The Hall voltage V_H can be positive and negative. But if one connects the sensor as follows (circuit 1):

Pin 1: positive input voltage V+, for instance +5VDC.
Pin 3: GND
Pin 2: OUTPUT
Pin 4: GND

One can only measure the positive voltage at the pin 2. This means that the output voltage at zero magnetic field is not zero. This voltage is called as offset voltage. The output voltage in this case is not equal to the Hall voltage. The output voltage is equal to the sum of offset voltage and Hall voltage.

The offset voltage will be zero if you connect double power supplies V+ and V- to the sensor (circuit 2):

Pin 1: positive input voltage V+, for instance +5VDC.
Pin 3: negative input voltage V-, for instance -5VDC
Pin 2: OUTPUT
Pin 4: GND

In this case the output voltage is equal to the Hall voltage.

Markt Schwabener Str. 8
D-85464 Finsing
Germany

Tel.: +49 (0)8121 – 2574100
Fax: +49 (0)8121– 2574101
Email: info@cy-sensors.com
http://www.cy-sensors.com

LM747 Datasheet

National Semiconductor

November 1994

LM747
Dual Operational Amplifier

General Description

The LM747 is a general purpose dual operational amplifier. The two amplifiers share a common bias network and power supply leads. Otherwise, their operation is completely independent.

Additional features of the LM747 are: no latch-up when input common mode range is exceeded, freedom from oscillations, and package flexibility.

The LM747C/LM747E is identical to the LM747/LM747A except that the LM747C/LM747E has its specifications guaranteed over the temperature range from 0°C to +70°C instead of −55°C to +125°C.

Features

- No frequency compensation required
- Short-circuit protection
- Wide common-mode and differential voltage ranges
- Low power consumption
- No latch-up
- Balanced offset null

Connection Diagrams

Metal Can Package

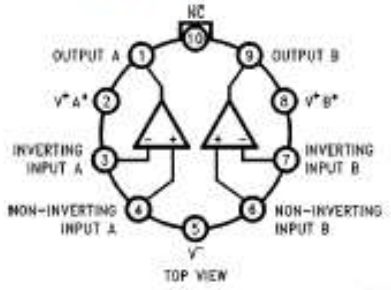

TL/H/11479–4

Order Number LM747H
See NS Package Number H10C

*V+ A and V+ B are internally connected.

Dual-In-Line Package

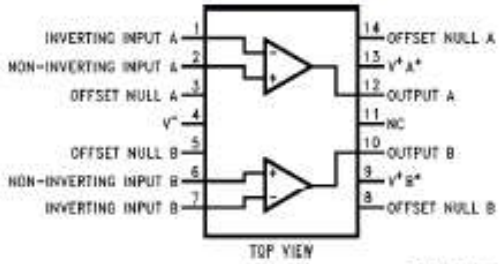

TL/H/11479–5

Order Number LM747CN or LM747EN
See NS Package Number N14A

Absolute Maximum Ratings

If Military/Aerospace specified devices are required, please contact the National Semiconductor Sales Office/Distributors for availability and specifications.

Supply Voltage	
LM747/LM747A	±22V
LM747C/LM747E	±18V
Power Dissipation (Note 1)	800 mW
Differential Input Voltage	±30V
Input Voltage (Note 2)	±15V
Output Short-Circuit Duration	Indefinite
Operating Temperature Range	
LM747/LM747A	−55°C to +125°C
LM747C/LM747E	0°C to +70°C
Storage Temperature Range	−65°C to +150°C
Lead Temperature (Soldering, 10 sec.)	300°C

Electrical Characteristics (Note 3)

Parameter	Conditions	LM747A/LM747E			LM747			LM747C			Units
		Min	Typ	Max	Min	Typ	Max	Min	Typ	Max	
Input Offset Voltage	$T_A = 25°C$ $R_S \leq 10\,k\Omega$ $R_S \leq 50\Omega$		0.8	3.0		1.0	5.0		2.0	6.0	mV
	$R_S \leq 50\Omega$ $R_S \leq 10\,k\Omega$			4.0			6.0			7.5	mV
Average Input Offset Voltage Drift				15							µV/°C
Input Offset Voltage Adjustment Range	$T_A = 25°C$, $V_S = \pm 20V$	±10				±15			±15		mV
Input Offset Current	$T_A = 25°C$		3.0	30		20	200		20	200	nA
				70		85	500			300	
Average Input Offset Current Drift				0.5							nA/°C
Input Bias Current	$T_A = 25°C$ $T_{AMIN} \leq T_A \leq T_{AMAX}$		30	80 0.210		80	500 1.5		80	500 0.8	nA µA
Input Resistance	$T_A = 25°C$, $V_S = \pm 20V$	1.0	6.0		0.3	2.0		0.3	2.0		MΩ
	$V_S = \pm 20V$	0.5									
Input Voltage Range	$T_A = 25°C$							±12	±13		V
		±12	±13		±12	±13					
Large Signal Voltage Gain	$T_A = 25°C$, $R_L \geq 2\,k\Omega$ $V_S = \pm 20V$, $V_O = \pm 15V$	50									V/mV
	$V_S = \pm 15V$, $V_O = \pm 10V$ $R_L \geq 2\,k\Omega$				50	200		20	200		V/mV
	$V_S = \pm 20V$, $V_O = \pm 15V$	32									V/mV
	$V_S = \pm 15V$, $V_O = \pm 10V$				25			15			V/mV
	$V_S = \pm 5V$, $V_O = \pm 2V$	10									V/mV
Output Voltage Swing	$V_S = \pm 20V$ $R_L \geq 10\,k\Omega$ $R_L \geq 2\,k\Omega$	±16 ±15									V
	$V_S = \pm 15V$ $R_L \geq 10\,k\Omega$ $R_L \geq 2\,k\Omega$				±12 ±10	±14 ±13		±12 ±10	±14 ±13		V
Output Short Circuit Current	$T_A = 25°C$	10 10	25	35 40		25			25		mA
Common-Mode Rejection Ratio	$R_S \leq 10\,k\Omega$, $V_{CM} = \pm 12V$				70	90		70	90		dB
	$R_S \leq 50\,k\Omega$, $V_{CM} = \pm 12V$	80	95								

Typical Performance Characteristics

Input Bias and Offset Currents vs Ambient Temperature

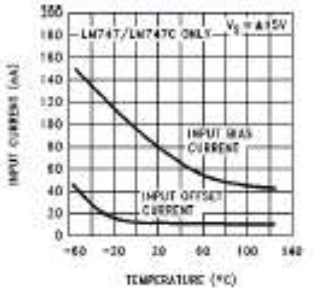

DC Parameters vs Supply Voltage

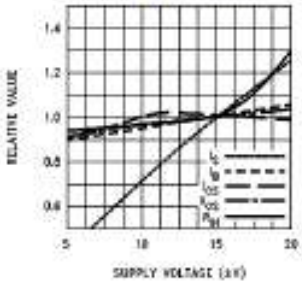

Common Mode Rejection Ratio vs Frequency

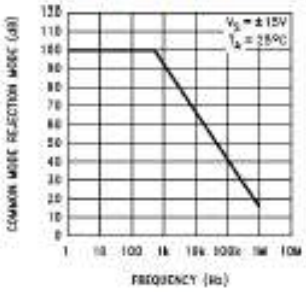

Output Voltage Swing vs Frequency

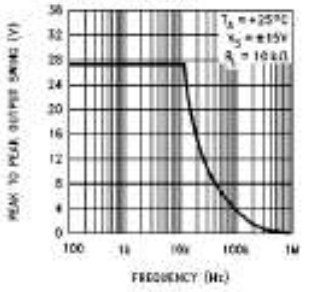

Output Voltage Swing vs Load Resistance

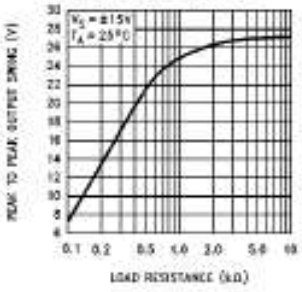

Output Swing and Input Range vs Supply Voltage

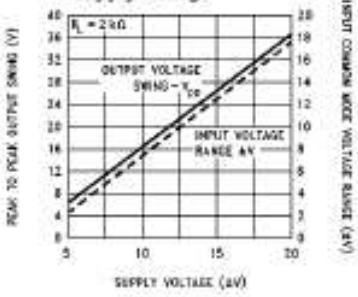

Normalized DC Parameters vs Ambient Temperature

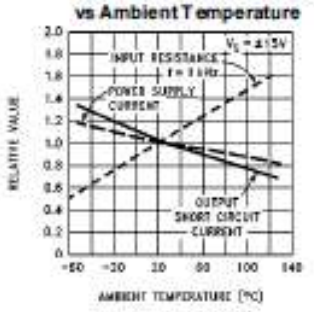

Transient Response

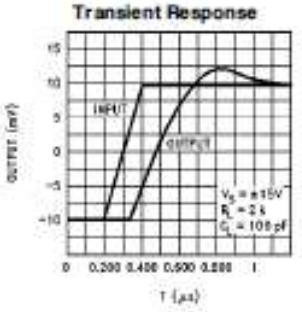

Frequency Characteristics vs Ambient Temperature

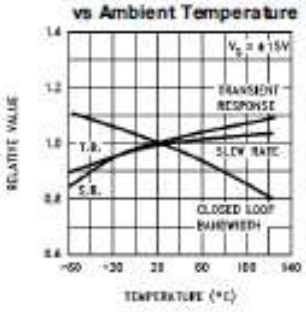

Frequency Characteristics vs Supply Voltage

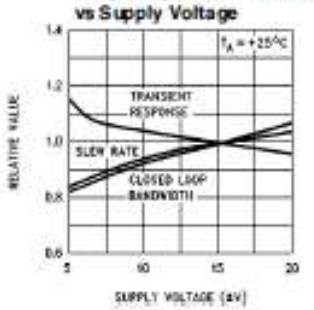

Output Resistance vs Frequency

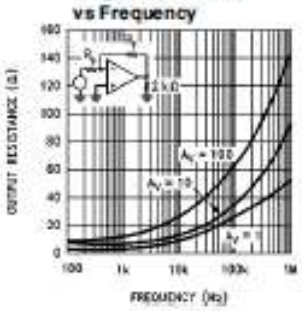

Open Loop Transfer Characteristics vs Frequency

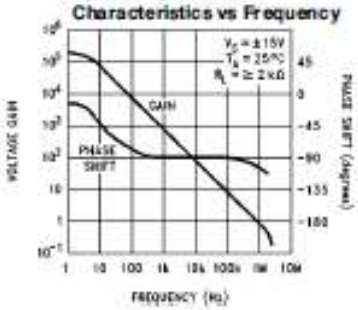

TL/H/11479–2

Physical Dimensions inches (millimeters) (Continued)

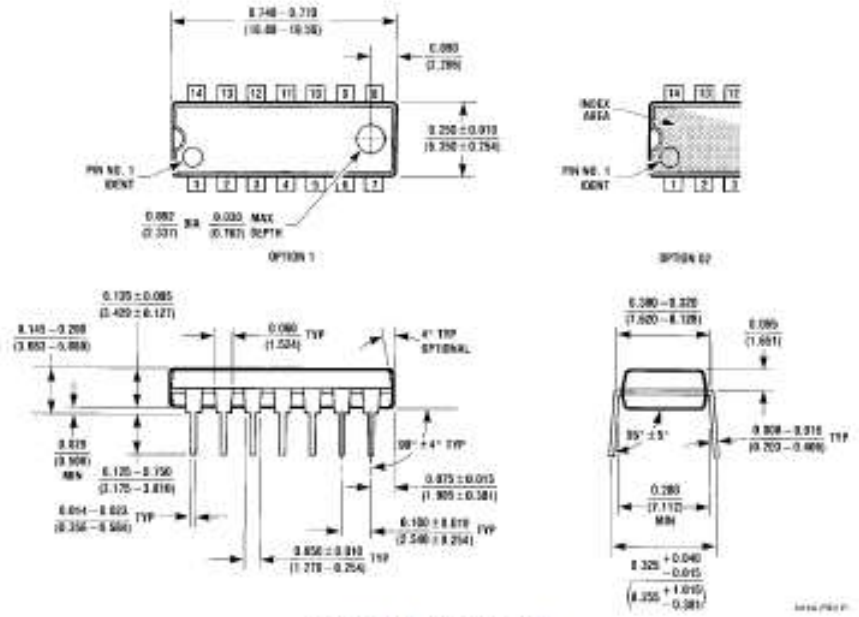

Dual-In-Line Package (N)
Order Number LM747CN or LM747EN
NS Package Number N14A

LIFE SUPPORT POLICY

NATIONAL'S PRODUCTS ARE NOT AUTHORIZED FOR USE AS CRITICAL COMPONENTS IN LIFE SUPPORT DEVICES OR SYSTEMS WITHOUT THE EXPRESS WRITTEN APPROVAL OF THE PRESIDENT OF NATIONAL SEMICONDUCTOR CORPORATION. As used herein:

1. Life support devices or systems are devices or systems which, (a) are intended for surgical implant into the body, or (b) support or sustain life, and whose failure to perform, when properly used in accordance with instructions for use provided in the labeling, can be reasonably expected to result in a significant injury to the user.
2. A critical component is any component of a life support device or system whose failure to perform can be reasonably expected to cause the failure of the life support device or system, or to affect its safety or effectiveness.

National Semiconductor Corporation
1111 West Bardin Road
Arlington, TX 76017
Tel: 1(800) 272-9959
Fax: 1(800) 737-7018

National Semiconductor Europe
Fax: (+49) 0-180-530 85 86
Email: cnjwge@tevm2.nsc.com
Deutsch Tel: (+49) 0-180-530 85 85
English Tel: (+49) 0-180-532 78 32
Français Tel: (+49) 0-180-532 93 58
Italiano Tel: (+49) 0-180-534 16 80

National Semiconductor Hong Kong Ltd.
13th Floor, Straight Block,
Ocean Centre, 5 Canton Rd.
Tsimshatsui, Kowloon
Hong Kong
Tel: (852) 2737-1600
Fax: (852) 2736-9960

National Semiconductor Japan Ltd.
Tel: 81-043-299-2309
Fax: 81-043-299-2408

MC14067B Datasheet

MC14067B

Analog Multiplexers / Demultiplexers

The MC14067 multiplexer/demultiplexer is a digitally controlled analog switch featuring low ON resistance and very low leakage current. This device can be used in either digital or analog applications.

The MC14067 is a 16−channel multiplexer/demultiplexer with an inhibit and four binary control inputs A, B, C, and D. These control inputs select 1−of−16 channels by turning ON the appropriate analog switch (see MC14067 truth table.)

Features

- Low OFF Leakage Current
- Matched Channel Resistance
- Low Quiescent Power Consumption
- Low Crosstalk Between Channels
- Wide Operating Voltage Range: 3 to 15 V
- Low Noise
- Pin for Pin Replacement for CD4067B
- These Devices are Pb−Free and are RoHS Compliant
- NLV Prefix for Automotive and Other Applications Requiring Unique Site and Control Change Requirements; AEC−Q100 Qualified and PPAP Capable

MAXIMUM RATINGS (Voltages Referenced to V_{SS})

Symbol	Parameter	Value	Unit
V_{DD}	DC Supply Voltage Range	− 0.5 to + 18.0	V
V_{in}, V_{out}	Input or Output Voltage Range (DC or Transient)	− 0.5 to V_{DD} + 0.5	V
I_{in}	Input Current (DC or Transient), per Control Pin	±10	mA
I_{sw}	Switch Through Current	±25	mA
P_D	Power Dissipation, per Package (Note 1)	500	mW
T_A	Ambient Temperature Range	− 55 to + 125	°C
T_{stg}	Storage Temperature Range	− 65 to + 150	°C
T_L	Lead Temperature (8−Second Soldering)	260	°C

Stresses exceeding Maximum Ratings may damage the device. Maximum Ratings are stress ratings only. Functional operation above the Recommended Operating Conditions is not implied. Extended exposure to stresses above the Recommended Operating Conditions may affect device reliability.

1. Temperature Derating:
   Plastic "P and D/DW" Packages: − 7.0 mW/°C From 65°C To 125°C

This device contains protection circuitry to guard against damage due to high static voltages or electric fields. However, precautions must be taken to avoid applications of any voltage higher than maximum rated voltages to this high−impedance circuit. For proper operation, V_{in} and V_{out} should be constrained to the range $V_{SS} \le (V_{in}$ or $V_{out}) \le V_{DD}$.

Unused inputs must always be tied to an appropriate logic voltage level (e.g., either V_{SS} or V_{DD}). Unused outputs must be left open.

ON Semiconductor®

http://onsemi.com

SOIC−24
DW SUFFIX
CASE 751E

MARKING DIAGRAM

A = Assembly Location
WL = Wafer Lot
YY = Year
WW = Work Week
G = Pb−Free Package

ORDERING INFORMATION

See detailed ordering and shipping information in the package dimensions section on page 5 of this data sheet.

ELECTRICAL CHARACTERISTICS

Characteristic	Symbol	V_{DD}	Test Conditions	−55°C Min	−55°C Max	25°C Min	25°C Typ [2]	25°C Max	125°C Min	125°C Max	Unit
SUPPLY REQUIREMENTS (Voltages Referenced to V_{SS})											
Power Supply Voltage Range	V_{DD}	–		3.0	18	3.0	–	18	3.0	18	V
Quiescent Current Per Package	I_{DD}	5.0 10 15	Control Inputs: V_{in} = V_{SS} or V_{DD}, Switch I/O: $V_{SS} \le V_{I/O} \le V_{DD}$, and $\Delta V_{switch} \le 500$ mV [3]	– – –	5.0 10 20	– – –	0.005 0.010 0.015	5.0 10 20	– – –	150 300 600	μA
Total Supply Current (Dynamic Plus Quiescent, Per Package	$I_{D(AV)}$	5.0 10 15	T_A = 25°C only (The channel component, $(V_{in} - V_{out})/R_{on}$, is not included.)	Typical			(0.07 μA/kHz) f + I_{DD} (0.20 μA/kHz) f + I_{DD} (0.36 μA/kHz) f + I_{DD}				μA
CONTROL INPUTS — INHIBIT, A, B, C, D (Voltages Referenced to V_{SS})											
Low–Level Input Voltage	V_{IL}	5.0 10 15	R_{on} = per spec, I_{off} = per spec	– – –	1.5 3.0 4.0	– – –	2.25 4.50 6.75	1.5 3.0 4.0	– – –	1.5 3.0 4.0	V
High–Level Input Voltage	V_{IH}	5.0 10 15	R_{on} = per spec, I_{off} = per spec	3.5 7.0 11	– – –	3.5 7.0 11	2.75 5.50 8.25	– – –	3.5 7.0 11	– – –	V
Input Leakage Current	I_{in}	15	V_{in} = 0 or V_{DD}	–	±0.1	–	±0.00001	±0.1	–	1.0	μA
Input Capacitance	C_{in}	—		–	–	–	5.0	7.5	–	–	pF
SWITCHES IN/OUT AND COMMONS OUT/IN — X, Y (Voltages Referenced to V_{SS})											
Recommended Peak–to–Peak Voltage Into or Out of the Switch	$V_{I/O}$	–	Channel On or Off	0	V_{DD}	0	–	V_{DD}	0	V_{DD}	V_{p-p}
Recommended Static or Dynamic Voltage Across the Switch [4] (Figure 1)	ΔV_{switch}	–	Channel On	0	600	0	–	600	0	300	mV
Output Offset Voltage	V_{OO}	–	V_{in} = 0 V, No Load	–	–	–	10	–	–	–	μV
ON Resistance	R_{on}	5.0 10 15	$\Delta V_{switch} \le 500$ mV [3], $V_{in} = V_{IL}$ or V_{IH} (Control), and V_{in} 0 to V_{DD} (Switch)	– – –	800 400 220	– – –	280 120 80	1050 500 280	– – –	1300 550 320	Ω
ΔON Resistance Between Any Two Channels in the Same Package	ΔR_{on}	5.0 10 15		– – –	70 50 45	– – –	25 10 10	70 50 45	– – –	135 95 85	Ω
Off–Channel Leakage Current (Figure 2)	I_{off}	15	$V_{in} = V_{IL}$ or V_{IH} (Control) Channel to Channel or Any One Channel	–	±100	–	±0.05	±100	–	±1000	nA
Capacitance, Switch I/O	$C_{I/O}$	–	Inhibit = V_{DD}	–	—	—	10	–	–	–	pF
Capacitance, Common O/I	$C_{O/I}$	–	Inhibit = V_{DD} (MC14067B) (MC14097B)	– –	– –	– –	100 60	– –	– –	– –	pF
Capacitance, Feedthrough (Channel Off)	$C_{I/O}$	– –	Pins Not Adjacent Pins Adjacent	–	–	–	0.47	–	–	–	pF

2. Data labeled "Typ" is not to be used for design purposes, but is intended as an indication of the IC's potential performance.
3. For voltage drops across the switch (ΔV_{switch}) > 600 mV (> 300 mV at high temperature), excessive V_{DD} current may be drawn; i.e. the current out of the switch may contain both V_{DD} and switch input components. The reliability of the device will be unaffected unless the Maximum Ratings are exceeded. (See first page of this data sheet.)

PACKAGE DIMENSIONS

SOIC–24 WB
CASE 751E–04
ISSUE F

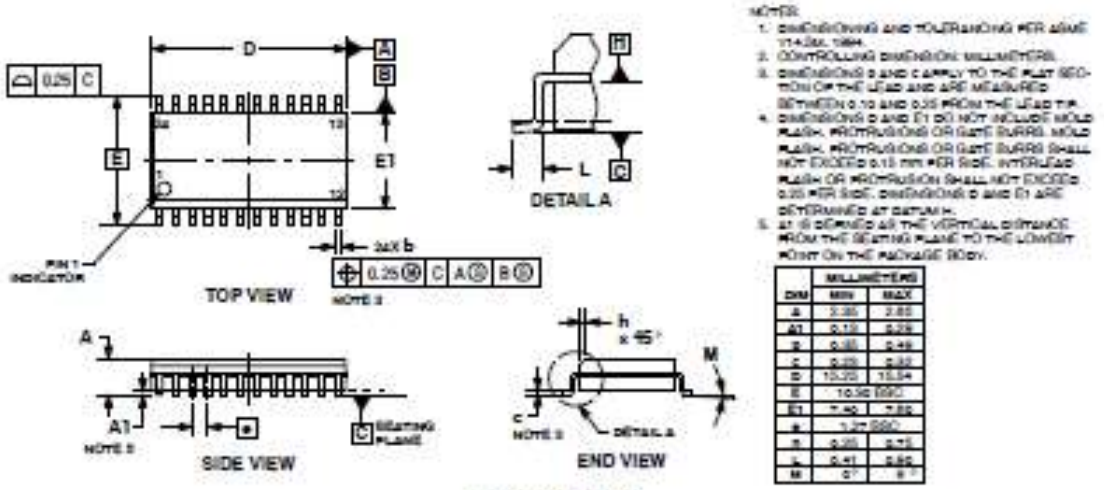

RECOMMENDED SOLDERING FOOTPRINT*

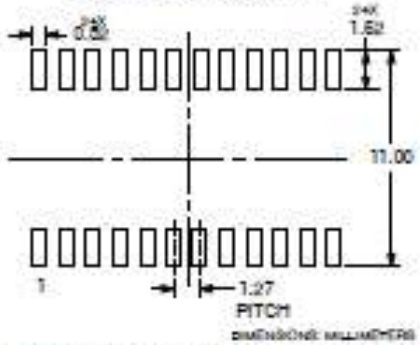

*For additional information on our Pb–Free strategy and soldering details, please download the ON Semiconductor Soldering and Mounting Techniques Reference Manual, SOLDERRM/D.

PUBLICATION ORDERING INFORMATION

LITERATURE FULFILLMENT:
Literature Distribution Center for On Semiconductor
P.O. Box 5163, Denver, Colorado 80217 USA
Phone: 303–675–2175 or 800–344–3860 Toll Free USA/Canada
Fax: 303–675–2176 or 800–344–3867 Toll Free USA/Canada
Email: orderlit@onsemi.com

N. American Technical Support: 800–282–9855 Toll Free USA/Canada
Europe, Middle East and Africa Technical Support:
Phone: 421 33 790 2910
Japan Customer Focus Center
Phone: 81–3–5817–1050

On Semiconductor Website: www.onsemi.com
Order Literature: http://www.onsemi.com/orderlit
For additional information, please contact your local Sales Representative

MC14067B/D

APPENDIX III

PUBLICATIONS

Paper submitted and presented at IETE 49th Mid Term Symposium-2018 held in Vishakhapatnam on 8th and 9th April, 2018

Challenges and research opportunities for future Internet

Rita roy[1], D Rajendra Dev[2], M Sreedevi[3], [1, 2,3]Department of Computer Science and Engineering, SANKETIKA Institute of Technology and Management, Visakhapatnam

Abstract: In multihop remote systems (MWNs), remote hubs can speak with each other through middle of the road hubs without the assistance of any framework. Along these lines, remote hubs are in charge of arranging and designing the system, and the administration of the system is dispersed between the hubs. Programming characterized organizing (SDN) is a promising arrangement, which decouples the control plane and the information plane to beat the difficulties of customary systems In this paper, we think about the advantages and the different perspectives of applying the SDN idea in MWNs (SDMWN). We first present MWNs, existing difficulties and the inspiration for applying SDN to such systems. At that point, in the wake of clarifying the SDN idea, we survey the related work in SDMWN. At long last, we talk about the difficulties in applying SDN and future research bearings in this zone.
Index Terms: Multihop remote systems (MWNs), programming characterized multihop remote systems administration (SDMWN), programming characterized organizing (SDN).

Design And Performance Analysis Of 2x1, 4x1 Rectangular Microstrip Patch Antenna Arrays For C Band, X Band, Ku Band Applications

[1]G.Ramalakshmi, [2] Prof. P.Mallikarjuna Rao, [1]Reasearch scholar, [2]Professor, Department of ECE, AU College of Engineering, Andhra University, Visakhapatnam-03

ABSTRACT: Multiresonant structure is one of the solution for broadband characteristics in patch antennas. Thin substrate materials with good dielectric constants are also favorable for such characteristics. In this paper the combination of E and U shaped slots on the patch antennas along with above mentioned substrate material properties are analyzed. In this work 2x1, 4x1 patch antenna arrays are considered, simulated and performance characteristics like Return loss, VSWR and radiation pattern are evaluated and the same are presented at the end. It is concluded that proposed antennas exhibited a wide bandwidth of 9.9GHz, 10.2GHz for 2x1 ,4x1 arrays respectively and are suitable for C Band, X Band, Ku Band Applications. The edge feed technique is used to simulate the single patch element, 2x1, 4x1 antenna arrays in the present work.

Key words: Antenna arrays, Edge Feed, Multiband and Broad Band, EU slot

HALL SENSOR ARRAY BASED MAGNETIC FIELD MEASUREMENT SYSTEM

Monika Budania[1], Annabelle Dani[1], Sanika Itagi[1], Lawansh Singh[1], B. Satyanarayana[2] and Amruta Pabarekar[1]
[1]Department of Electronics and Telecommunication, Fr. C.R.I.T, Vashi, Navi Mumbai, India
[2]Department of High Energy Physics, Tata Institute of Fundamental Research, Colaba, Mumbai, India
Email: 1lawansh10@gmail.com, 2bsn@tifr.res.in

Abstract: Measurement of magnetic fields is one of the important requirements in many research and development applications. Hall Sensors which function on the principle of Hall Effect, are used to measure these parameters. In this paper, we propose a Hall sensor array based magnetic field measurement system. 16 hall sensors are mounted on a thin mount equidistant to each other at a gap of 60 mm and their sensing element being parallel to the mount. While on the front-end, the sensor signals are multiplexed and amplified, they are digitised and processed by a microcontroller on the back-end. A suitable graphical user interface is also developed to customise and control the system as well to output and archive the data suitably. We will present the motivation of our work and describe the design along with selection criteria of various chosen sensors and other components. We will also discuss about our initial results obtained along with future prospects of our work.

Keywords: Magnetic field, Hall Sensor, INO project, Data acquisition system.

Hall Sensor Array based Magnetic Field Measurement System

Monika Budania[1], Annabelle Dani[2], Sanika Itagi[3], Lawansh Singh[4], B. Satyanarayana[5] and Amruta Pabarekar[6]
[1, 2, 3, 4, 6]Department of Electronics and Telecommunication, Fr. C.R.I.T, Vashi, Navi Mumbai, India
[5]Department of High Energy Physics, Tata Institute of Fundamental Research, Colaba, Mumbai, India
Email: [1]monikabudania999@gmail.com, [2]annabelle.dani97@gmail.com, [3]sanikaitagi@gmail.com, [4]lawansh10@gmail.com, [5]bsn@tifr.res.in, [6]amruta.pabarekar@fcrit.ac.in

Abstract-- **Measurement of magnetic fields is one of the important requirements in many research and development applications. Hall Sensors which function on the principle of Hall Effect, are used to measure these parameters. In this paper, we propose a Hall sensor array based magnetic field measurement system. 16 hall sensors are mounted on a thin mount equidistant to each other at a gap of 60 mm and their sensing element being parallel to the mount. While on the front-end, the sensor signals are multiplexed and amplified, they are digitised and processed by a microcontroller on the back-end. A suitable graphical user interface is also developed to customise and control the system as well to output and archive the data suitably. We will present the motivation of our work and describe the design along with selection criteria of various chosen sensors and other components. We will also discuss about our initial results obtained along with future prospects of our work.**

Keywords-- **Magnetic field, Hall Sensor, INO project, Data acquisition system.**

I. INTRODUCTION

Magnetic field vector is a force generated by moving electric charges currents and calculated using the Ampere's Law or the Biot-Savart Law. When describing it inside magnetised materials which themselves contribute to internal magnetic fields, this field is denoted by either magnetic flux density, B (Tesla) or magnetic field strength, H (amperes per meter). Magnetic field is one of the two components of the Electromagnetic force, which is one of the most pervasive fundamental forces of nature. Magnetic fields are most commonly applied in working of modern technologies and designing instrume*nts. Motors and generators, electromotive instruments and mass transport systems, navigation devices and material handling equipments are some of the examples.

While in everyday life, magnetic fields created by permanent magnets are most often encountered, magnets of different kinds - electromagnetic, superconducting etc., are being extensively used in experimental nuclear and high energy physics and material sciences. Very large and powerful magnets are used to build particle accelerators and detectors typically to accelerate or bend the charged particle beams and measure the energy of the particles. Magnetic forces give information about the charge carriers in a material through the Hall Effect. And on the other hand, Hall Effect is often exploited to precisely measure and monitor magnetic field strengths of all the magnetic systems mentioned above, which is an important requirement of such systems.

II. MOTIVATION

The India-based Neutrino Observatory (INO) is a multi-institutional national project aimed at building a world-class underground laboratory at the Bodi West Hills near Madurai in Tamil Nadu. The collaboration is deeply engaged in design and construction of a mega science experiment called Iron Calorimeter (ICAL) for studying many key open questions involving the elusive particles called neutrinos. The magnetised ICAL will consist of more than 50000 tons of iron plates arranged in stacks with gaps in between where around 28,800 Resistive Plate Chambers (RPCs) would be inserted as active detectors. A total of about 3.6 million ultra high speed detector signals need to be instrumented in this detector [1].

One of the most important capabilities of the ICAL detector is to distinguish between positively and negatively charged particles produced by the neutrinos within the ICAL detector as well as measure their energies. In fact, ICAL will be world's largest electromagnet, which is built using the iron plates and copper coils. About 1.5 Tesla magnetic field which will be produced within the ICAL will bend the particles of opposite polarities in different directions, hence identifying their charge. Also By measuring the radius of curvature of these bent tracks, one can estimate the momentum or energy of the particles. We therefore need precise simulation

of the field within the volume of the detector as well as its measurement.

It is proposed by the INO collaboration that a prototype ICAL detector of 4m x 4m x 11 layers and weighing about 85 tons be built in IICHEP laboratory in Madurai to facilitate initial experiments related to magnet construction and other concerned issues. A picture of this magnet under construction is shown in Figure 1. Construction scheme of the magnet along with iron plates and copper coils is clearly seen in the picture.

Figure 1: Magnet of the prototype ICAL detector under installation and commissioning in Madurai.

Simulated magnetic flux in a layer of the prototype detector using the configuration shown in Figure 1 is given in Figure 2. The design criteria is that we achieve more than 1 Tesla field in as large a volume (about 90%) as possible using minimum current in the Copper coils.

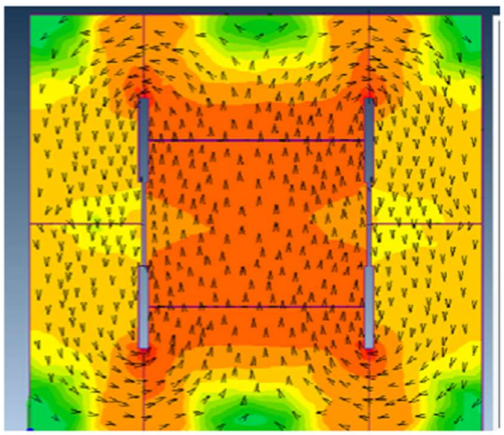

Figure 2: Simulated magnetic flux lines in an iron layer of the the prototype detector.

It was strongly desired by the Collaboration that a reliable and versatile measurement system may be developed for insitu monitoring the magnetic field in the prototype detector of the ICAL. Specially designed Hall sensor arrays are planned to be inserted or mounted in the gaps of size 1000mm x 56mm x 3mm available in the structure. It is envisaged that such a system, if found suitable and useful may also be deployed for the ICAL detector itself by replicating a large number of these systems. Table 1 lists specifications of the measurement system [2].

Parameter	Value
Basic Sensor Material	Mono-crystal GaAs
Type of Probe	For transverse field measurement
Measurement Range	Upto 30 KGauss
Accuracy	0.2% of full scale
Non Linearity	<1%
Maximum Input current/voltage	30 mA/10 V
Max input power	150 mW
Operating Temp. Range	40-150 °C
Hall output voltage at B=100mT, I=8 mA, V=6V	110-150 mV
Offset Voltage	±11 mV
Input Resistance	650-800 Ω
Output Resistance	650-800 Ω
Temperature Coefficient of Hall output voltage	0.06%/°C
Temperature Coefficient of Hall output resistance	0.3%/°C

Table 1: Hall probe sensor specifications.

III. Literature Review

Magnetic sensors are used for converting magnetic field into electrical signals [3]. Magnetic sensors have many applications such as position tracking and navigation systems, detection of ferromagnetic and conducting objects and antitheft systems. Possible magnetic field measurement methods found in the literature are induction based (flux meter and flux gate), Hall Effect based, magneto resistance based, magnetic resonance based and super conducting quantum interference device (SQUID) based. But methods like SQUID come under low field sensors which can sense very low values of magnetic fields, i.e., under 1μGauss. Hall sensors have very wide range, good accuracy and a very wide bandwidth, so they were chosen as the primary sensors for magnetic field measurement system for the ICAL prototype detector.

Most commonly used magnetic sensors are MEMS-type, which are bigger in size. In this project, size of the probe is of major concern, where the thickness of the mount including the sensor should fit into a slot of less than 3mm. Therefore a Hall sensor is chosen. A hall sensor is a type of magnetic sensor

whose output is a function of magnetic field density. It is based on the principle of Hall Effect, discovered in 1879 by Edwin Hall. The Hall Effect is favored in materials with high electron mobility and low conductivity. Hence, in a Hall sensor, the base material used is a semiconductor and not a metal [4].

When a conductor is placed in a magnetic field perpendicular to the direction of the electrons, they will be deflected from a straight path. Therefore, one plane of the conductor becomes positively charged and the side opposite to this becomes negatively charged. The voltage between these planes is called the Hall voltage. This output Hall voltage is given by the following equation:

$$V_h = R_h \left(\frac{I}{t} \times B \right)$$

Where:

- V_H is the Hall voltage in Volts
- R_H is the Hall Effect co-efficient
- I is the current flow through the sensor in Amperes
- t is the thickness of the sensor in mm
- B is the magnetic flux density in Tesla

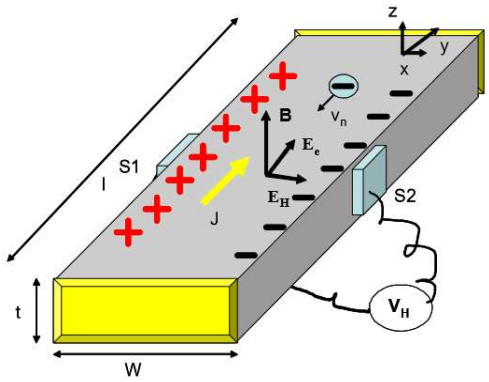

Figure 3: Illustration of Hall Effect [4].

Hall Effect is illustrated in Figure 3. A magnetic field B (normal to the plate) is applied and a current I (current density J) flows in the y direction through the CC contacts. The output voltage is measured through the S1S2 contacts. Hall Effect sensors in the market are available with either linear or digital outputs. The output signal for linear sensors is taken directly from the output of the operational amplifier. In case of linear output Hall Effect sensors, as the strength of the magnetic field increases the output signal from the amplifier will also increase until it begins to saturate. The saturation voltage is limited by the supply voltages. Digital output sensors on the other hand use a Schmitt trigger circuitry connected to the operational amplifiers. When the magnetic flux passing through the Hall sensor exceeds a preset value, the output from the device switches quickly between its "OFF" condition to an "ON" condition.

A market survey was conducted to identify Hall sensors which match the design specifications and the same are shortlisted in the Table 2.

Parameter	CYSJ106C	CYSJ166A	KSY14
Basic sensor Material	Mono-crystal GaAS	Mono-crystal GaAS	Mono-crystal GaAS
Hall Output Voltage, mV B=100mT, IC=8mA/VC=6V	110-150	156-204	95-130
Offset Voltage, mV	±11	±8	±20
Input Resistance, Ω	650-850	1000-1500	900-1200
Output Resistance, Ω	650-850	1800-3000	900-1200
Maximum input current/voltage	13mA/10V	12V	7mA
Operating Temp. range	-40-125°C	-40-125°C	-40-175°C

Table 2: Summary of Hall sensors meeting the system requirement specifications.

IV. Overview of the System

The measurement system essentially comprises of three major subsystems, namely the signal acquisition, analog and digital signal processing and front end data and user interface. Figure 4 shows block diagram of the hardware part of the magnetic field measurement system.

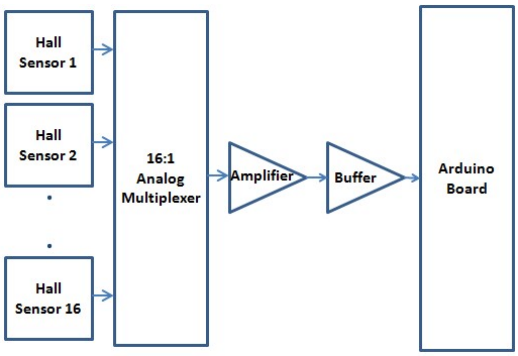

Figure 4: Block diagram of the hardware of the magnetic field measurement system.

The signal acquisition subsystem senses the magnetic field at multiple points in and converts it into corresponding analog voltages. This is essentially achieved by the network of a 16 Hall

sensors, which in turn are fed to the subsequent analog and digital signal processing subsystems. Here the signals from 16 Hall sensors are multiplexed and the multiplexed signal is amplified by an operational amplifier (LM747N) based amplifier. This data is further sent to an inbuilt Analog to Digital Converter (ADC) of a microcontroller for digitizing the sensor signals. An analog buffer (LM747N) was used to provide impedance matching and driving capability to the amplified signal from the multiplexer board to the microcontroller board. Overall control, readout and communication with the front end user interface are achieved a commercial microcontroller board.

Thus, this subsystem works on the principle of Time Division Multiplexing, wherein one sensor at a time is selected by the microcontroller using select lines of the analog multiplexer (CD4067N) and its data is processed in a continuous loop.

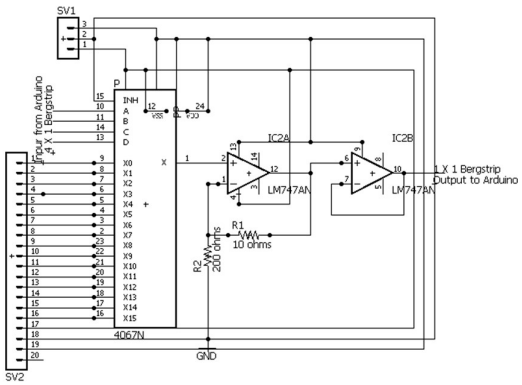

Figure 5: Multiplexer-Amplfier-Buffer module.

The multiplexer-Amplifier-Buffer module of the project was implemented as shown in Figure 5 and the performance parameters of the same matched with the expected results. The result was observed on an Arduino board's Serial Monitor. For the signal conditioning stage, the Hall sensor outputs were simulated by multiple voltages supplied from DC power supplies. The output of these power supplies were set to a few volts, similar to the voltage output expected from the Hall sensors. The readings measured by a digital multimeter matched accurately with those obtained by the Arduino IDE board.

The front-end GUI refreshes the display screen with the acquired data after a fixed time. The multiplexing avoids need for one ADC channel of the microcontroller per sensor, instead only one ADC channel is sufficient for all the 16 sensors. This design methodology is suitable for this system as the signals produced by the sensor even during ramp up or ramp down of magnetic field are very slow and are essentially DC signals. Therefore multiplexing of the sensors or the some finite amount of time taken for processing of data for per sensor doesn't affect the performance of the overall system.

V. Hardware Design

As mentioned previously the Hall sensor array will be inserted in an inter-iron plate gap of 1000mm x 56mm x 3mm within the detector volume. This arrangement is schematically depicted for a single sensor in Figure 6.

On one end of the same PVC strip, mounted another small PCB which housed the analog multiplexer and a linear amplifier circuits. A flat cable that ran from the small PCB across all the sensor boards distributes the bias voltages to the sensors and brings sensors' output signals to the analog multiplexer. The small PCB takes power supplies through an appropriate connector, sends out the multiplexed and amplified signal to the ADC through a LEMO connector and also receives the digital I/O lines for sensor selection on a flat cable from the microcontroller board.

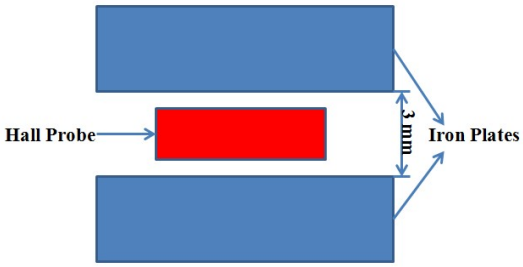

Figure 6: Schematic of sensor position and placement in the detector.

The following design methodology of the sensor array is followed to satisfy the system requirements. A PVC strip of 1000mm x 55 mm is chosen as shown in the upper part of Figure 7. It was sliced in its thickness in order to hold the tiny sensor pitch adapter boards without increasing the overall thickness of the probe. The sensor boards are placed at the centre of the PVC strip and at about 60mm distance from each other and 16 such sensor boards are mounted on the PVC strip as shown in the lower part of Figure 7. This design allows placing of sensors precisely at the middle position of the iron plate thickness (which is 55mm) vertically while making measurements. A perpendicular extension is designed on the PVC strip for hand grip so that the 1000mm long strip can be inserted and removed easily.

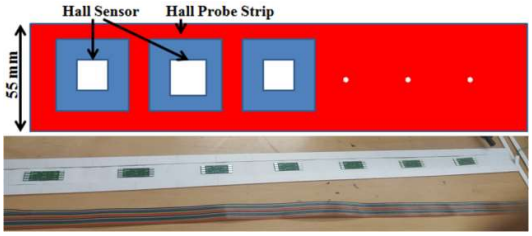

Figure 7: Schematic of the Hall probe array (upper part) and fully assembled probe (bottom part).

Overall thickness of the sensor array strip is maintained at 2mm, thus leaving about 0.5mm on its either side to wrap with an insulating plastic film before inserting the strip inside a gap between iron plates. The insulating film will also provide protection to the probe against any scratches, damages and dust.

Thus two types of PCBs - one sensor board (16 nos.) and another of multiplexer and amplifier board (one no.) were used to fabricate the sensor array strip. Schematics for both the boards were prepared, which were then used to prepare the layout using OrCAD. Double sided design was used to prepare and produce both the PCBs without any manufacturing problems with high reliability and performance.

VI. SOFTWARE DESCRIPTION

The data acquisition software selects sensors in a loop, acquires statistically significant number of readings for each sensor, applies corresponding calibration of the sensor, presents the data in a convenient format to the user and finally stores the data on disk as per the user requirement for later retrieval and analysis. National Instruments Labview software platform was used to design an elegant Graphical User Interface (GUI) that performs all the above mentioned functions of the system. A inbuilt functionality called VISA resource was made use of in order to communicate with the microcontroller using a serial USB communication port. The software essentially consists of two main windows, a block diagram and a front panel. The block diagram window is used to create serial read logic from the microcontroller using VISA resource manager (as shown in Figure 8). Front panel is used for displaying various indicators and graphs, The readings can also be imported into a spreadsheet for detailed analysis purposes later.

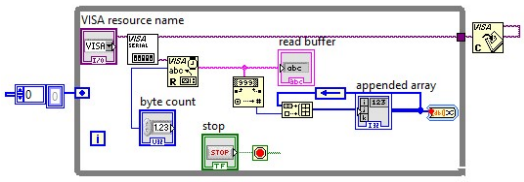

Figure 8: Block diagram of the Labview Software. The sensor readings are obtained sequentially via the serial port and displayed on the front panel.

Similarly the front end of the probe was built using Labview and corresponding fields appeared in front panel. Shown in Figure 9 is a sample code run by the microcontroller module and readings obtained on the front panel.

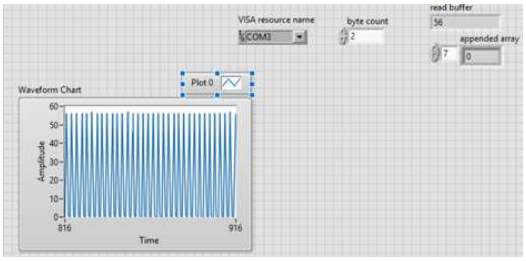

Figure 9: Front panel of Labview, showing readings obtained on analog pin of arduino, and serially transmitted to the Labview via serial USB.

VII. PRELIMINARY RESULTS

To begin with, the system was tested qualitatively by using a pair of permanent magnets. The plot in Figure 10 shows as the distance between two permanent magnets increases, the hall voltage decreases. But magnetic field intensity increases as distance decreases. Therefore, we can conclude that hall voltage is directly proportional to magnetic field intensity and inversely proportional to the distance between magnets.

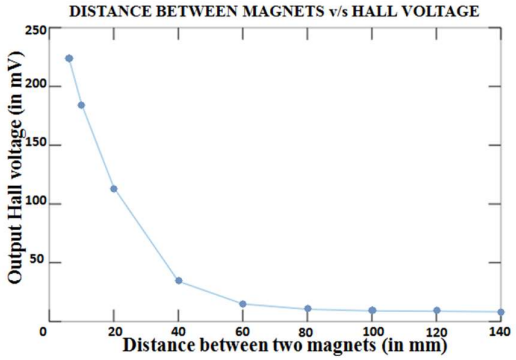

Figure 10: Qualitative testing of the system using a pair of permanent magnets.

We followed this measurement by systematically studying relative performance of the two Hall probe sensors - CYSJ106C and CYSJ166A that we procured. A summary of these studies are shown in Table 3.

SNo.	Measurement Conditions	Output Voltage (in mV)
1	One pair of magnets	CYSJ106C - 40.9mV
2	Two pairs of magnets	CYSJ106C - 116.3mV
3	One pair of magnets with two Hall sensors kept side by side	CYSJ106C - 31.1mV CYSJ166A - 41.6mV

Table 3: Comparative performance study of two of the Hall sensors.

In Test Condition 1, a pair of magnets with a stronger magnetic field were placed 45mm apart. The CYSJ106C sensor was placed between the two magnets. The output was found to be 40.9mV. In Test Condition 2, the first pair of stronger magnets were placed in the same position as that in Condition 1 and a pair of weaker magnets were placed 65cm apart. The sensor CYSJ106C was placed exactly in the middle of both pairs of magnets. The output voltage was found to be 116.3mV. In Test Condition 3, a single pair of magnets were used with two sensors (CYSJ106C and CYSJ166A) placed side by side. The reading obtained by CYSJ106C was 31.1mV while it was 41.6mV with CYSJ166A. Based on these observations and the specifications given, we conclude that CYSJ106C is better suited for our requirements than CYSJ166A.

After the initial studies reported above, a probe was assembled using six sensors initially. This was a full system mockup in which the Hall probes, the electronics (multiplexing and amplification), ADC, microcontroller and front-end software components all were tested. Two sets of readings were taken to verify reproducibility of the system. Table 4 shows the readings taken without and with magnetic field, which show reasonable consistency at this stage of the project.

Cha. No.	Reading 1 (in mV)		Reading 2 (in mV)	
	Without Magnets	With Magnets	Without Magnets	With Magnets
2	120	660	120	660
4	210	620	210	640
6	160	700	170	700
8	210	660	210	680
10	120	600	120	620
12	170	560	180	540

Table 4: Test results of reproducibility studies of the Hall sensor array.

VIII. CONCLUSIONS AND FUTURE SCOPE

A probe based on 16 Hall sensors for making insitu measurements of precise magnetic field inside the prototype ICAL detector was designed, built and characterised. Further precision and precise calibration studies of the system using a standard will be carried out immediately. The probe will be populated with full set of 16 sensors soon. Various functionalities in the front-end user GUI for data presentation and storage will be coded. The probe will be deployed in the prototype ICAL detector, which is being installed and commissioned soon at IICHEP laboratory, Madurai and measurements will be taken. Long term stability studies on the detector magnetic field will be also performed using this probe and the results will be supplied to the INO collaboration. Performance of this system will be studied before going ahead with production of a large number of units meant for future versions of the ICAL detector.

ACKNOWLEDGEMENTS

Authors would like to express their deep sense of gratitude the INO collaboration for providing us with this wonderful opportunity to carry out our project work at TIFR, Mumbai and for designing this useful instrument meant for deployment in an actual high energy physics experiment. We would also sincerely thank Shri S.R.Joshi for his contributions to this project and other members of the collaboration for all their help and suggestions. Support of the Department of Electronics and Telecommunication, Fr. C.R.I.T, Vashi throughout this work is gratefully acknowledged.

REFERENCES

[1] India-based Neutrino Observatory – INO website, http://www.ino.tifr.res.in

[2] N.S.Dalal, S.Ajith, Sandip Patel, Saurabh Pathak, S.P.Prabhakar, Development of Magnetic Measurement System for Mini ICAL Magnet for INO Project, DRHR, BARC, Mumbai

[3] Hall Effect Sensor – Electronics Tutorials Online, http://www.electronics-tutorials.ws/electromagnetism/hall-effect.html

[4] S.Sanfilippo, Hall probes: physics and application to magnetometry, CERN-2010-004, pp. 423-4

References

[1] Online: India-based Neutrino Observatory – INO website
[Available]: http://www.ino.tifr.res.in

[2] Online: All about Neutrinos
Available: http://icecube.wisc.edu/outreach/neutrinos

[3] Online: Neutrino – Wikipedia
Available: https://en.wikipedia.org/wiki/Neutrino

[4] Online: Hall effect – Wikipedia
Available: https://en.wikipedia.org/wiki/Hall_effect

[5] Online: Lorentz force – Wikipedia
Available: https://en.wikipedia.org/wiki/Lorentz_force

[6] Online: Hall Effect Sensor – Electronics Tutorial
Available: http://www.electronics-tutorials.ws/electromagnetism/hall-effect.html

[7] S. Sanfilippo, Paul Scherrer Institute, Villigen, Switzerland
Hall probes: physics and application to magnetometry
Available: https://cds.cern.ch/record/1334470/files/423.pdf

[8] Online: Hall Effect Sensor and How Magnets Make It Works
Available: www.electronics-tutorials.ws › Electromagnetism

[9] Online: Hall effect sensor – Wikipedia
Available: https://en.wikipedia.org/wiki/Hall_effect_sensor

[10] N.S. Dalal, S. Ajith, Sandip Patel, Saurabh Pathak, S. P. Prabhakar, *Development of Magnetic Measurement System for Mini ICAL Magnet for INO* Project Division of Remote Handling & Robotics, Bhabha Atomic Research Centre, Mumbai-400085.

[11] Online: Proteus Design Suite – Wikipedia
Available: https://en.wikipedia.org/wiki/Proteus_Design_Suite.

[12] Online: 'Eagle Reference',
Published.
Available: http://www.autodesk.com/products/eagle/overview

[13] Online: OrCAD - Wikipedia
Available: https://en.wikipedia.org/wiki/OrCAD

[14] Online: Introduction to Graphical Programming with LabVIEW By Jeffrey Travis and Jim Kring Oct 27, 2006
Available:
http://www.informit.com/articles/article.aspx?p=662895&seqNum=3

[15] Online: 'Arduino References',
Published.
Available: http://www.arduino.cc [Accessed: February 2017]

[16] Online: ‘MC14067B datasheet’.
Published.
Available: https://www.onsemi.com/pub/Collateral/MC14067B-D.PDF

[17] Online: ‘LM 747 datasheet’.
Published.
Available: http://www.ti.com/lit/ds/symlink/lm747.pdf

[18] Online: 'Arduino datasheet',
Published.
Available: https://datasheet.octopart.com/A000066-Arduino-datasheet-38879526.pdf

[19] Online: Atmega 328 pinout
Available:http://www.learningaboutelectronics.com/Articles/Atmega328-pinout.php

[20] Online: Accelerator Based Atomic Physics Laboratory Department of Nuclear and Atomic Physics,TIFR
Available: http://www.tifr.res.in/~abap/ecr.html

[21] Online: 'CYSJ106C datasheet',
Published.
Available: http://www.hallsensors.de/CYSJ106C.pdf

Acknowledgement

This project would not have been possible without the kind support and help of many individuals. We would like to express our deep sense of gratitude to the INO collaboration for providing us with this wonderful opportunity to carry out our project work at TIFR, Mumbai and for designing this useful instrument meant for deployment in an actual high energy physics experiment. We are highly indebted to Professor B. Satyanarayana, Project Mentor Department of High Energy Physics, Tata Institute of Fundamental Research, Colaba, Mumbai for his ongoing guidance, supervision and suggestion as well as for providing necessary information and the approach towards our project with a lot of patience and faith. We would also sincerely thank Shri S.R. Joshi (DHEP, TIFR), Ms. Darshana Gonji (DHEP, TIFR), Mr. K.V Thulasi Ram (DNAP, TIFR), Prof. Lokesh Tribedi (DNAP, TIFR), Prof. S. N Mishra (DNAP, TIFR) and Mr. Chandan Bagdia (DNAP, TIFR) for their contributions to this project and for all their help and suggestions. We would like to thank Ms. Amruta Pabarekar, Project Mentor FCRIT Vashi, Navi Mumbai for her valuable guidance and feedback in the scope of this project.

We would like to express our gratitude towards our Project Coordinator, Prof. Keerthi Unni, Head of the Department Dr. Milind Shah and all the professors of EXTC Department for their unending support, encouragement and suggestions. Our special thanks to Mumbai University for inclusion of Project in our curriculum giving a trigger to our young minds by providing an opportunity to work on this project and enhance our team work capabilities.

Last but not the least, the team, thanks each member for contributing to the project with the best of their abilities and all those who have directly or indirectly contributed to the success and completion of our project.

THANK YOU

Annabelle Dani

Monika Budania

Sanika Itagi

Lawansh Singh